DOE/JPL 954355/78-3
Distribution Category UC-63

Mobil Tyco Solar Energy Corporation
16 Hickory Drive
Waltham, Massachusetts 02154

LARGE AREA SILICON SHEET BY EFG

Program Manager: F.V. Wald

Annual Progress Report - Subcontract No. 954355

Covering Period: October 1, 1977 - September 30, 1978

February 16, 1979

(NASA-CR-158379) LARGE AREA SILICON SHEET BY EFG Annual Progress Report, 1 Oct. 1977 - 30 Sep. 1978 (Mobil Tyco Solar Energy Corp.) 79 p HC A05/MF A01 CSCL 10A
N79-20483
Unclas
G3/44 16681

"The JPL Low-Cost Silicon Solar Array Project is sponsored by the U.S. Department of Energy and forms part of the Solar Photovoltaic Conversion Program to initiate a major effort toward the development of low-cost solar arrays. This work was performed for the Jet Propulsion Laboratory, California Institute of Technology by agreement between NASA and DOE."

ABSTRACT

During the fiscal year 1978, on which we report here, progress in EFG ribbon growth was made in a number of areas as follows:

1. Multiple growth for ribbons 5 cm in width was demonstrated in two runs of 12 and 20 hours' duration.

2. A new single cartridge crystal growth station, designated Machine 17, was built. It has vastly expanded observational capacity by virtue of an anamorphic optical-video system which allows close observation of the meniscus over 7.5 cm in width, as well as video taping of the ribbon growth process for further analysis. Also, a number of mechanical advances were incorporated into this equipment.

3. Growth Station No. 1 achieved reproducible and reliable growth of 7.5 cm wide ribbon at speeds up to 4 cm/min.

4. A major advance in cartridge design, the "mini cold shoe", was introduced.

5. Interface shaping using the "displaced-die" concept led to significant increases in cell efficiency. Large area cells (2.5 by 7.5 cm^2, 2.5 x 10 cm^2, and 7.5 by 7.5 cm^2), which achieve efficiencies over 9%, have been made in significant numbers.

6. The role of gaseous impurities in cartridge furnaces has been clarified and their destabilizing influence on growth has been brought under control.

Details of most of these developments are discussed in the report.

Table of Contents

PRECEDING PAGE BLANK NOT FILMED

List of Figures

List of Figures (continued)

List of Tables

I. INTRODUCTION

At the beginning of the fiscal year on which this document reports, it was well established that EFG material, in spite of its imperfect nature, is quite capable of producing large area (2.5 x 10 cm^2) solar cells with efficiencies of at least 12%. Indeed, the discussion of whether small area cells of higher efficiency could conceivably be prepared from some of the material, had already been shifting to the question of defining the influence of particular defects on the overall yield of cells prepared from whole multiple meter lengths of ribbon, and attempts to prepare single cells with optimized properties were de-emphasized.

Instead, under this contract the focus shifted to considering even larger cells (5 x 10 cm^2 and 7.5 x 7.5 cm^2) prepared from 5 cm and 7.5 cm wide ribbon, grown under conditions which would make high rate multiple ribbon growth a practical reality. The characterization task, therefore, took more and more of an interest in questions related to uniformity of properties over very large cell areas and within long ribbons, instead of concerning itself with the top performance of selected small ribbon areas.

Thus, the program in its philosophy shifted to engineering research, i.e., answering questions related to specific machine design elements; the ribbon quality to be expected from growth stations built in certain ways and using particular materials of construction, and the relations between silicon ribbon quality and productivity; i.e., such questions as to how speed and width affect the ribbon properties both from a mechanical (flatness, thickness uniformity, etc.) and solid-state (in the end, solar cell efficiency) standpoint.

Overall, we believe that this programmatic approach has been successful and that a realistic engineering concept has been proven which will allow the achievement of high ribbon productivity along with good ribbon quality and thus low solar cell blank cost. Specifically, major achieve-

ments of the program which support this statement are:

1. The soundness of the engineering concepts has been demonstrated by the achievement of multiple (five) ribbon growth for periods up to 20 hours.

2. Significantly improved single ribbon equipment using a cartridge (Machine 17) has been constructed on schedule this year. It provides unique capabilities for studying and understanding the growth process itself as well as a simple basic concept for automatic feedback control.

3. The work on JPL Machine No. 1 (MTSEC No. 18) has led to the design of highly reliable growth cartridges in which experiments of 7.5 cm wide growth can be conducted in a reproducible manner, i.e., when one sets out to grow a ribbon, one can actually grow as much as a full crucible allows every time. During the last three months, this equipment operated on a regular schedule of two one-day runs per week, without any significant parts failure.

4. The introduction of the so-called "mini cold shoe" represents a major advance in reliable cartridge design.

5. A concept that had been proposed for some time, namely to use specific interface shaping to improve material properties of wide ribbon, has finally been reduced to practicability by the use of displaced dies. This has led to solar cells (in sizes of 2.5 x 10 cm^2, 2.5 x 7.5 cm^2, and 7.5 x 7.5 cm^2) grown from a reliable, practical cartridge system which have average efficiencies of over 9% in random lots of ~10 pieces. Most importantly, the material is indeed asymmetrical as predicted, not only with respect to solar cell efficiency but also with respect to silicon carbide density.

Thus, enough understanding of the effects has been gained to make further advances in this area quite likely so that the solar cell efficiency in these large ribbon cells is expected to reach similar averages which are now obtained in cells made from smaller ribbons.

6. Detailed studies of the effect of the gaseous environment in an EFG furnace have led to the discovery that growth stability can be significantly enhanced and SiC density can be greatly reduced by proper atmosphere control.

However, before final production machine prototype design can begin, the various approaches which have been derived need still to be optimized and made ready for fully automatic operation at high growth rates, a fact

that becomes clearly apparent from the detailed discussions in the text that follows. In particular, the main hurdle toward higher growth rates, namely the buckling that produces unacceptable, non-flat ribbon, has to be overcome and the approaches toward higher cell efficiencies have to be refined so that they are more effective and can be combined with high growth rates (> 5 cm/min).

Experiments which generate the needed basic facts in these areas can, however, be conducted now in an optimum way, since both direct observational tools (Machine 17) and sufficient basic understanding of the details of the growth process are available. We are thus confident that the final prototype design of a ribbon production machine could begin within a year.

II. WORK ON CRYSTAL GROWTH STATION NO. 1 by J.P. Kalejs

A. Overview

The past year of experimentation on JPL No. 1 has seen the attainment of a number of important milestones in the development of a high speed 7.5 cm ribbon growth system capable of producing material of acceptable solar cell quality. Foremost in significance has been the achievement of reliable growth of 7.5 cm wide ribbon. This has been aided by identification of thermal conditions promoting ribbon edge stability and their implementation through the use of a new design of end heater. The availability of reliable growth 7.5 cm cartridges and consistently reproducible growth conditions is indispensable to furthering understanding of factors which affect ribbon quality. This understanding has contributed to the realization of improvement in performance of large area (nominal 7.5 cm by 7.5 cm) solar cells by a factor of about two, from below 5% initially to over 9% (AR coated, under AM1 conditions) most recently. Equally as important, the experiments have helped identify parameters which have to be controlled if additional improvements in material quality are to be achieved. These results and the areas of future work will be examined in more detail below.

Recognition of the necessity to control the level of contaminating gases in the argon furnace atmosphere in order to improve growth stability has led to the installation in JPL No. 1 of auxiliary gas feed tubes. The argon overpressure in the neighborhood of the growth interface produced by this extra gas flow has effectively decoupled the cartridge atmosphere from that in the main furnace. One immediate benefit has been to allow growth from quartz crucibles under conditions essentially indistinguishable from those achieved with graphite crucibles by preventing SiO from reaching the neighborhood of the growth interface and cold shoe in amounts great enough to affect growth conditions.

Examination of material grown from JPL No. 1 suggests that both the capillary feed and die top geometries can be used to manipulate impurities in the melt ahead of the growth interface before they are incorporated into the growing ribbon. Die designs which utilize central capillary melt feeds have been fabricated and used to explore the feasibility of using fluid flow to redistribute impurities in the ribbon width dimension in a manner beneficial to material quality improvement. Improvement attributable to favorable redistribution effects is observed for growth of 3 to 4 cm wide ribbon at speeds up to and of the order of 3 cm/min. The benefits of impurity redistribution are not so easily discernible for wider ribbon and/or higher speed growth. Experiments are being planned to attempt to exploit this effect further in the latter growth regimes.

In the second area of investigation of the possibility of impurity manipulation in the melt, dies have been deliberately made asymmetric in the thickness cross-section in an attempt to influence the interface shape in this dimension. One such change, a uniform displacement of one die flat with respect to the other, across the full width of the die, has resulted in striking asymmetry in ribbon surface characteristics, as well as solar cell quality, with respect to the two faces of the ribbon. The ribbon face growing from above the low side of the die top (with the higher meniscus) is virtually free of silicon carbide and smooth in appearance. Solar cells made using this surface for the junction side have efficiencies of the order of 9% (AM1 and AR coated). On the other hand, the SiC particle density is generally moderate to high (1 to 10 particles per cm^2) on the surface growing from above the high die (low meniscus) side. Solar cells made using this surface are poor, with efficiencies generally less than 5% (AM1 and AR coated).

At this point, there is not sufficient evidence to relate differences in solar cell performance and observed SiC particle density asymmetry to interface shape changes and deliberately introduced growth asymmetry. Identification of the factors which are responsible for material quality improvement effected by any impurity manipulation in the melt is complicated by the interdependence of many relevant parameters in a given system with acceptable growth conditions. Future experiments with capillary and die top geometry design variations will attempt to better define the limits of solar cell improvement that can be achieved in the 7.5 cm cartridge system.

One of the goals for the 7.5 cm cartridge system is the attainment

of growth speeds of 7.5 cm/min. The information on material quality obtained to date, to which the above remarks apply, has come from material grown at speeds between 2.5 and 4.5 cm/min. In this speed range, ribbon buckling is at tolerable levels insofar as material handling and processing yields are concerned. Now that considerable progress in improving material quality has been made for lower speed growth, the study of buckle formation and the effect of increases in growth speed on material quality can proceed with more confidence. Preliminary results indicate that changes in interface shape and in the manner in which fluid flow affects impurity redistribution in the melt ahead of the growth interface can be expected with increases in growth speed, even in the speed range covered to date. Further experiments are being planned in this area. Buckle characterization, with respect to type, amplitude and period, will also be initiated for ribbon grown in this lower speed range in conjunction with work on JPL No. 3A and Furnace 17.

B. Crystal Growth

1. Experimental

The furnace chamber was given a thorough cleaning, new main zone furnace components installed, and cartridges completely disassembled and rebuilt with clean components in preparation for the second series of clean runs started this quarter. Two molybdenum gas flow tubes feeding the interior of the cartridge were installed. These terminate at the level of the die heaters and are designed to provide control of the gas environment near the growth interface as well as help decouple the cartridge atmosphere from that of the main furnace. In another area, improvements have been made in the mounting of the belt puller to the cartridge to reduce the possibility of ribbon misalignments during growth.

A summary of growth runs made in this quarter is given in Table I. Three separate 7.5 cm cartridge assemblies have been brought into operational status in order to facilitate the study of the effects of a number of design variations in cartridge components on growth performance and material quality. Two of these employ all-molybdenum cold shoes, one with a 0.15 cm and the other with a 0.32 cm cold shoe spacing. The third cartridge contains a stretched version of the 5 cm stainless steel cold shoe blocks in use in JPL No. 3A. The latter provides extra flexibility of experimentation in that heat removal elements of several thicknesses and openings are available as attachments for use with the cold shoe blocks. Except for the cold shoe assemblies, most other cartridge compo-

Table I. Run and Ribbon Data for JPL No. 1.*

Run No.	Speed Range (cm/min)	Length (m)	Comments
18-89	-	-	No growth possible; main zone power failure.
18-90	3.6 - 4.0	5.3	First test of displaced die with 0.050 cm top slot and 0.012 cm displacement. Undoped melt, clean conditions, all-molybdenum cold shoe. Central saw cut capillary die.
18-91	3.2 - 4.0	2.2	Baseline run with standard multicapillary die. First run of second clean series; melt doped to 1 Ω-cm.
18-92	3.5 - 3.8	1.8	Standard setup with regular multicapillary die. Second run of clean series.
18-93a	-	-	No growth possible due to water leak in cartridge.
18-93b	3.0 - 3.5	0.9	Repeat of 18-92. Growth limited by die misalignment.
18-94	-	-	Stretched version of 5 cm cartridge cold shoe, last used in run 18-48. Cartridge assembly error, no growth possible.
18-95	3.5 - 4.2	2.3	Fourth run of series. Displaced saw cut die; 0.050 cm top slot, 0.025 cm displacement. Full width growth not possible due to end instabilities.
18-96	3.5 - 4.6	6.1	Displaced saw cut die; 0.012 cm displacement on 0.025 cm top slot. Some instability in growth attributed to air leak; mostly narrow ribbon grown. All molybdenum cold shoe, 0.15 cm spacing.
18-97	3.0 - 4.6	3.8	Displaced central capillary die; 0.007 cm displacement on 0.050 cm top slot. Stretched version of 5 cm cold shoe, 0.15 cm spacing. Growth instabilities limit widths to 3 - 5 cm. Suspect air leak in helium line.
18-98	3.6 - 3.8	2.5	Radius multicapillary die; undoped melt, cold shoe as in 18-97. No helium flow to cartridge.
18-99	2 - 3.5	2.9	Repeat of 18-98 with doped melt, increased cold shoe spacing (0.32 cm). No helium flow to cartridge.
18-100	2.5 - 3.5	4.8	Central capillary die; no displacement, 0.050 cm top slot. No helium flow to cartridge. All molybdenum cold shoe (0.32 cm spacing).
18-101	2 - 3.5	2.1	Displaced central capillary die; same as in run 18-96. No helium flow to cartridge. Cold shoes as in 18-100.
18-102	2.2 - 3.1	4.0	Displaced central capillary die and 1 Ω-cm doped melt; crucible emptied with single seeding (no freezes) in over two hours of continuous growth. Over 90% of ribbon was full width.

*All growth was from graphite crucibles.

nents are interchangeable among the cartridges. More frequent cleaning and re-baking of cartridge components is thus feasible without suffering an inordinate amount of down time, with the added possibility that this procedure may also help decrease the level of contaminants in the growth system with time.

The main emphasis in the experiments carried out the past quarter has been to determine whether improvements in material quality could be realized by growth from a displaced die. This die differs from the standard die used in that one die top flat is "displaced", or lowered, deliberately with respect to the other across the full width of the die, as shown in Fig. 1(a). The expectation was that the growth interface shape across the ribbon thickness would be sensitive to such a die top asymmetry, which would create unbalanced heat fluxes to the die top through the differing cross-sectional areas of the die top flats. A possible meniscus configuration in the thickness cross-section for growth from the displaced die, shown in end view in Fig. 1(a), is depicted in Fig. 1(b).

A number of runs were made with displaced dies, differing in die top slot width and extent of displacement, to explore the limits of growth afforded without modifications to other cartridge components. Two widths of die top slot were tried, 0.025 cm and 0.050 cm, each with displacements of 0.012 and 0.025 cm. Several runs with regular dies were interspersed among the displaced die runs to monitor baseline cartridge and material quality performance. The displaced die configuration which gave the most stable growth was one with a 0.012 cm displacement on a 0.050 cm wide die top slot. Two runs were made with this die. Run 18-90 was undoped and run 18-102 was doped to the regular level of 1 Ω-cm, p-type. Exceptionally stable growth was achieved in the latter. Only one seeding was required, as the crucible was emptied of melt without a single freeze occurring in over two hours of continuous, full-width growth.

Full-width growth with all the displaced die variations tested was noticeably less stable than with non-displaced dies. Even though growth conditions in the best of cases (those of the most successful runs, 18-90 and 18-102) were acceptable, the ribbon could not be left unattended for more than a few minutes without experiencing drift of the ribbon edge. Full-width growth was not possible with the most extreme die displacements that were used in run 18-95. Ribbon edge position control became noticeably more difficult in all cases as growth speed was increased. The most stable growth of runs 18-90 and 18-102 was realized at speeds

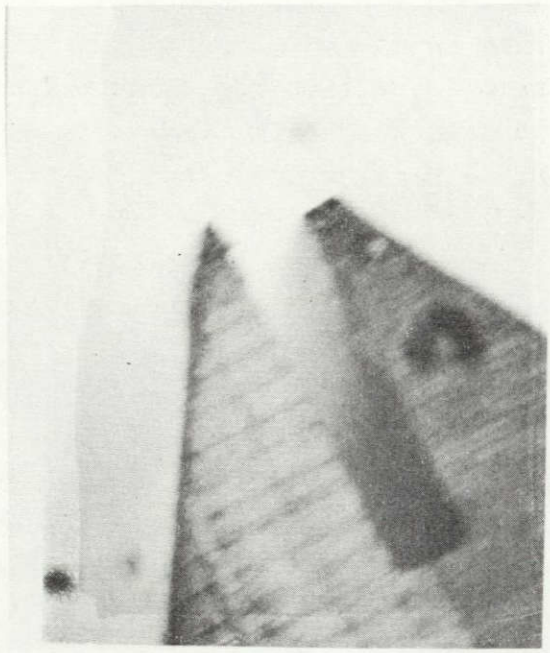

(a)

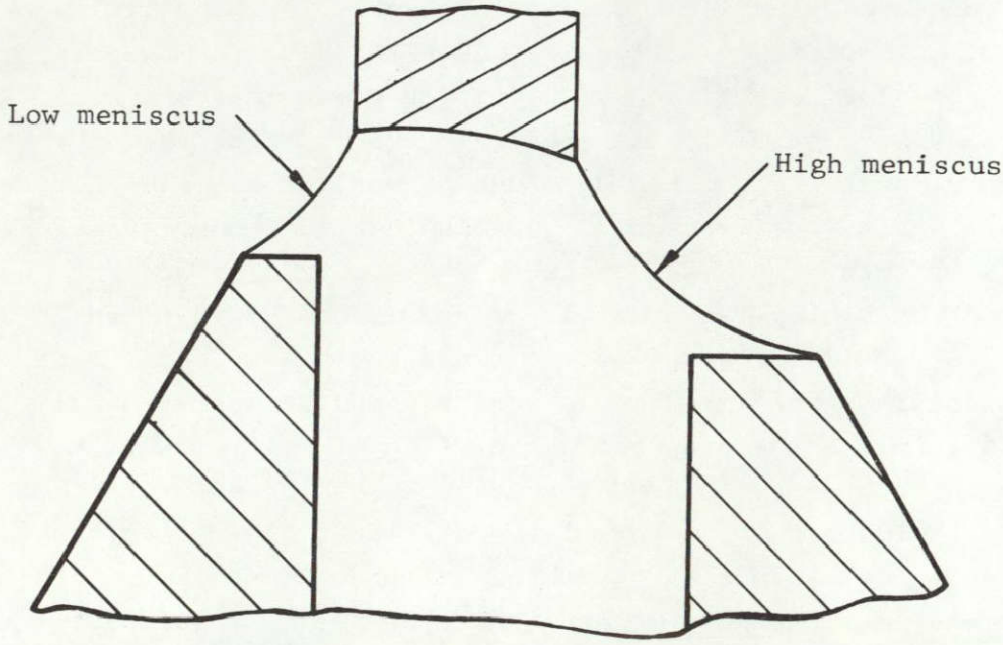

(b)

Fig. 1. Displaced die: (a) end view photograph, and (b) meniscus configuration showing possible interface shape.

below about 3.5 cm/min.

A striking feature of growth observed for all the displaced dies used was an asymmetry in the SiC particle density with respect to the two faces of the ribbon. The ribbon surface growing from above the high meniscus (displaced) side of the die was exceptionally shiny and virtually free of SiC particles. On the other hand, the density on the low meniscus side was much higher in all instances. This asymmetry persisted under all extremes of growth conditions (e.g., speed, ribbon width) encountered in the displaced die runs.

The above experiments with displaced dies have helped define limits of stable growth that can be expected from a system in which only a uniform displacement of one die flat is made in the manner described. On the basis of the limited information obtained to date, it appears that in order to achieve stable growth with displacements greater than about 0.012 cm, further system component modifications will be required. Two possibilities which will be explored are: (1) shaping of the die top in addition to the displacement to attempt to increase the range of meniscus heights available for stable growth, and (2) alteration to other cartridge components (face heater, die shields, cold shoes) so as to help compensate thermally for the die top asymmetry introduced through the displacement.

2. Material Quality Considerations

The task of improving the quality of ribbon grown from the 7.5 cm high speed cartridge has received top priority on JPL No. 1 over the past eight months. A considerable amount of data has been gathered in the course of two series of clean runs. Interpretation of this data is made difficult as a result of the complexity of the growth system, with interdependence among many growth parameters and cartridge components. In addition, there is a degree of uncertainty associated with a given set of experimental data obtained in a developmental system such as this because of unavoidable changes in component design and operating procedures made in the course of time. Nevertheless, certain trends in the data are emerging; these will be discussed in the context of the improvements in material quality which have been achieved.

The results for solar cells made from ribbon grown in the most recent clean runs are given in Table IX (Section IV). The best performance cells to date for 7.5 cm cartridge material were obtained in run 18-102 (see also Table II). Both the average AM1 cell efficiency of 9.4%

Table II. Cell Parameters for Displaced Die Runs in JPL No. 1. Cell Junctions are Made from the High Meniscus Side Ribbon Face, Scribed in Strips 2.5 cm by 7.5 cm, with the Longer Dimension Along the Full Ribbon Width, Except as Noted (no AR Coating).

Cell No.	Area (cm^2)	I_{rv} (mA/cm^2)	V_{oc} (V)	I_{sc} (mA/cm^2)	FF	P (mW/cm^2)
18-96-1	15.20	0.127	0.489	15.49	0.611	4.63[2]
-2	17.40	0.011	0.514	16.61	0.749	6.39
-3	16.17	0.066	0.514	16.81	0.724	6.26
-4	15.20	0.254	0.513	16.56	0.725	6.17
-5	17.05	0.012	0.518	16.60	0.685	5.89
-7[1]	25.50	0.038	0.498	14.92	0.740	5.46
-8[1]	25.50	0.117	0.509	15.80	0.728	5.85
-9[1]	25.50	0.643	0.408	13.00	0.423	2.24[2]
-10[1]	25.55	0.008	0.501	15.03	0.720	5.42
-11[1]	25.47	0.016	0.500	14.93	0.743	5.48
-12[1]	25.55	0.008	0.499	15.10	0.741	5.58
-13[1]	18.67	0.052	0.423	10.99	0.497	2.31[2]
-14[1]	18.45	0.011	0.497	15.30	0.729	5.55
-15[1]	18.15	0.266	0.456	11.49	0.546	2.86[2]
-16[1]	15.95	0.091	0.507	15.87	0.747	6.01
-17[1]	14.65	0.014	0.488	13.45	0.646	4.24[2]
18-97-1	14.75	0.014	0.513	15.93	0.746	6.10
-2	15.00	0.096	0.512	16.69	0.727	6.21
-3[1]	12.00	0.016	0.505	14.67	0.747	5.50
-4[1]	25.40	0.038	0.517	16.68	0.735	6.34
-5[1]	25.35	0.114	0.521	17.25	0.736	6.61
-6[1]	25.07	0.058	0.513	16.02	0.727	5.98
-7[1]	25.33	0.114	0.509	16.02	0.684	5.57
-8[1]	25.35	0.095	0.496	14.58	0.660	4.77[3]
-9[1]	22.77	0.170	0.500	14.50	0.642	4.66[3]
-10[1]	17.77	0.081	0.505	16.13	0.671	5.46
-11[1]	16.13	0.010	0.520	16.82	0.732	6.40
18-102-1	18.25	0.011	0.524	17.01	0.691	6.15
-2	18.23	0.011	0.530	16.91	0.716	6.42
-3	18.30	0.237	0.530	16.83	0.718	6.41
-4	18.13	0.011	0.530	16.86	0.700	6.26
-5	18.19	0.292	0.534	16.94	0.714	6.45
-6	14.23	0.014	0.533	17.88	0.696	6.63
-8	18.25	0.396	0.526	16.13	0.714	6.06
-9	18.20	0.318	0.527	16.97	0.694	6.21
-10	18.12	0.106	0.532	17.27	0.724	6.65
-11	18.20	0.026	0.535	18.08	0.718	6.95
-12	18.18	0.053	0.527	17.36	0.728	6.66

1. Cells made from narrow ribbon ($\leq$ 4 cm wide), nominal 2.5 cm by 10 cm size, with the longer dimension along the growth direction.
2. Low meniscus side surface used for cell junction.
3. Higher speed growth at 4.6 cm/min.

Dies: 18-96 - 0.025 cm top slot, .012 cm displacement, saw cut.
18-97 - 0.025 cm top slot, .007 cm displacement, central capillary.
18-102 - 0.050 cm top slot, .012 cm displacement, central capillary.

and the narrow spread in cell parameters represent significant improvements over performance levels achieved in earlier runs. Although the contribution of specific factors to better cell performance cannot be deduced from the available data, certain changes made in the crystal growth procedure have had noticeable effects. The following discussion will concentrate on examining the data relating to the influence of growth conditions on solar cell performance. These results fall into two categories: observations relating to the desirability of control over the furnace and cartridge atmospheres, and the effect of die design and growth conditions on material quality.

a. Atmosphere Control

Auxiliary argon flow to the cartridge was introduced at the start of the second series of clean runs (with run 18-90) in an effort to achieve better control over the atmosphere in the neighborhood of the growth interface and growing ribbon. This has been found to be desirable because of observations that contamination of the argon atmosphere by deliberately introduced oxygen, as well as naturally occurring gases (SiO and CO, particularly when growth from quartz crucibles was attempted), had undesirable effects on growth stability and cartridge performance.[1] The current gas flow configuration introduces additional argon to the cartridge just below the die shields and close to the level of the die top and meniscus. The overpressure which is achieved at flow rates of the order of 10 ℓ/min is designed to inhibit furnace gases from entering the cartridge, while at the same time providing a more constant flow past the interface and up the growth slot. (The only gas flow to the cartridge before this modification had been through the cold shoe. This rate was varied frequently during a run to assist in growth.) The contributions of this arrangement in furthering material quality, although not demonstrable at this time, are thought to be significant. By aiding in the attainment of more reliable and reproducible growth, the frequency of successful seeding and ease of constant width growth increases. This, in turn, reduces contamination of the die top by silicon spills and SiC particle build-up. A second possible benefit relates to the establishment and maintenance of a more inert atmosphere surrounding the meniscus and growing ribbon. This replaces, to a great extent, the furnace ambient, which is more likely to contain volatile oxides of elements detrimental to ribbon quality.

b. Die Design Considerations

Theoretical studies of impurity transport mechanisms in the melt contained by the die[2] and experimental results from growth runs made in JPL No. 3A[3,4] have suggested that die design could have an important influence on the manner in which impurities are incorporated into the crystal during EFG of silicon ribbon. For the dies currently used to grow 5 cm and 7.5 cm wide ribbon, the system effective distribution coefficient for impurities is unity in the sense that all impurities which enter the die capillaries must end up in the growing ribbon (neglecting impurity exchange with the die material and atmosphere). For a given level of impurity contamination of the bulk melt, it is, therefore, advantageous to find a means by which impurity levels in the melt adjacent to the interface can be manipulated in order to minimize their deleterious effect on material quality. The feasibility of accomplishing this by convective redistribution and/or interface shape modification has been addressed as part of the series of clean runs in JPL No. 1.

As a result of encouraging preliminary experiments,[3] a study of the effect of die capillary geometry on growth conditions and material quality was incorporated into the first series of clean runs, runs 18-65 to 18-88. Three different melt flow configurations were investigated. The die top cross-sections illustrating these are shown in Fig. 2. The multicapillary and central capillary designs represent cases where the effect of convective impurity transport in the melt is predicted to be quite different. In the former, impurities should be swept to regions between capillaries, thus depleting the areas above the capillary exit; in the latter, they are expected to be swept toward the ribbon edges. Material from the ribbon edge is removed during cell processing; if it has a higher average impurity content, then the net effect on cell performance should be beneficial. The central saw cut die in Fig. 2 represents an intermediate case, in which lateral redistribution of impurities across the ribbon width is expected to take place but not to as great an extent as for the central capillary arrangement.

The results of the initial experiments demonstrating the effects of die design on material quality carried out with the 5 cm cartridge system in JPL No. 3A have been already presented.[3,4] To summarize briefly, expected improvement in material quality above a capillary exit was demonstrated in one run (16-087) during growth of 3 to 4 cm wide ribbon at about 3 cm/min from a single central capillary die.[3] Cell efficiencies of above 12% (AR coated) were achieved on small mesa diodes

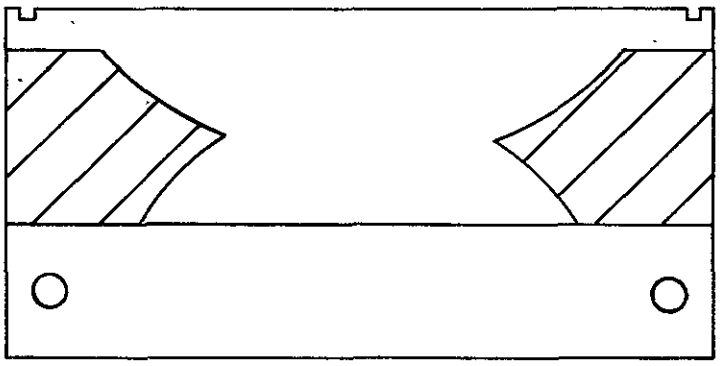

(a)

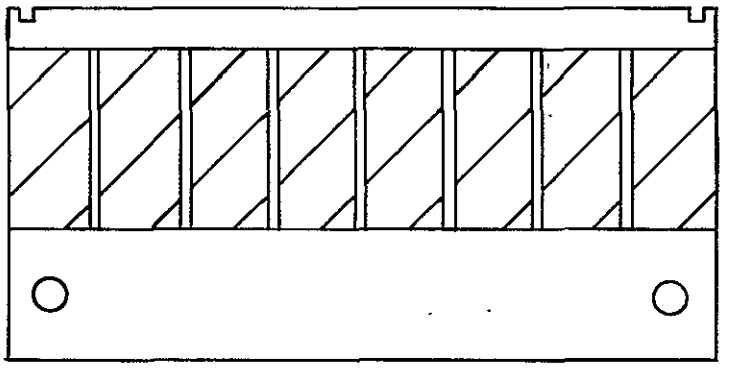

(b)

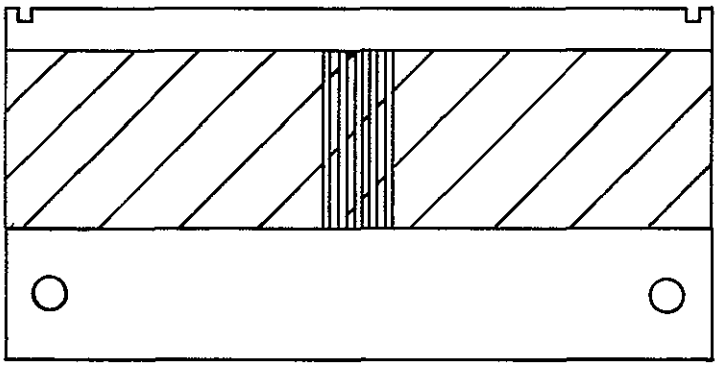

(c)

Fig. 2. Cross-sections of die configurations: (a) central saw cut die, (b) multicapillary die, and (c) central capillary die.

($\lesssim 0.1$ cm^2 in area), with large area cells having efficiencies of better than 10%. However, due to less than ideal growth conditions and asymmetric SiC particle densities on the ribbon surfaces, these results could not be reproduced in a second experiment (run 16-090), although the influence of a die capillary geometry change on material quality was again observed. Additional experience gained in runs in JPL No. 1 now indicates that the SiC particle asymmetries and non-reproducibility of results were most likely caused by poorly machined die tops, which produced an effect much like the displaced dies described above. The recent data also suggest that an interrelation between melt flow patterns and interface shape may complicate interpretation of results. This connection will be explored further in discussions below.

During tests of multicapillary and central capillary die designs in runs 18-65 to 18-79, the inadequacy of these types of capillary flow arrangements in producing satisfactory and reproducible growth became increasingly evident. Cross-sectioning of the die top showed that individual capillaries very often became blocked partially or entirely through SiC crystal growth from the inside walls of the capillaries. The extent of this growth was not predictable. In one extreme case, growth from a single capillary die was terminated abruptly after one meter of ribbon was pulled under initially excellent growth conditions (run 18-78). Cross sections of the capillary revealed a dense SiC crystal growth at the die top, which appeared to be responsible for the growth failure.

The unpredictable partial or entire capillary blockage by SiC growth is evidently very undesirable from the point of view of studying and understanding the effects of melt impurity transport ahead of the growth interface. This problem also extends into the area of growth stability. It is not known for what level of SiC crystal growth constriction of melt flow will be serious enough to disrupt lateral flow when central capillary die geometries are used, thus reducing capillary driving forces (i.e., increasing the h_{eff}) and leading to meniscus height instabilities at the ribbon edges. This is felt to be of particular concern in cartridge growth, where an already large h_{eff} makes further increases undesirable and potentially disruptive to growth.

Several steps have been taken to attempt to alleviate the problem of capillary blockage by SiC. The concentration of SiC crystals at the capillary exits to the die top slot (see Fig. 2) suggested that one of the contributing factors to excessive SiC growth in this region was the abrupt change in cross-section in going from a circular vertical capillary

to a rectangular die top slot. The change in cross-section, by itself, would distort flow streamlines and lead to regions of separated flow in and around the juncture. The regions of quiescent fluid thus formed could then be a more favorable place for growth of SiC particles.

Abrupt changes in capillary cross-section are avoided in the central saw cut die (see Fig. 2), in which the entire capillary is of the same cross-section. This die design has been used in a number of runs and has shown excellent reliability in producing acceptable growth. The effect of going to this melt flow configuration on material quality has not been evaluated to date. The period over which this die was tested (runs 18-80 to 18-88) was also one in which attempts to introduce oxygen into the ribbon were being made.[1] Growth conditions were quite often unpredictable on this account, and solar cell performance was inconsistent (see Table IX, Section IV). The available results appear to indicate that this die design will be helpful in avoiding the SiC crystal growth problem associated with the other capillary geometries. In addition, this design allows a considerable flexibility in the alteration of the capillary geometry through the use of different combinations and depths of the saw cuts used to form the capillary. A continuation of its use will be resumed in coming runs.

Growth of SiC also occurs on other capillary surfaces in contact with the molten silicon, with a large variability in the density and size of crystals. Of particular concern in connection with studies of impurity redistribution across the ribbon width is the growth of SiC in the die top slot and on the die top flats. The potential disruptive influence of this SiC growth has been partially negated by use of dies with increased width die top slots: 0.050 cm as against 0.025 cm. This also allows growth from a higher meniscus and avoids much SiC particle pickup from the die top. However, it does not circumvent the problem completely, as larger SiC particles generally are found to be present and blocking the lateral melt flow path to a greater or lesser extent. The perturbative effect of their presence could be expected to become more noticeable with increasing ribbon width when central capillary die designs are used.

c. Impurity Redistribution in the Melt

The data gathered from the initial runs with displaced dies have provided new impetus in the study of mechanisms of impurity transport in the melt during EFG. This has come about on two accounts. First, this die allows growth of ribbon with one face which is virtually

free of SiC and therefore smoother relative to material grown from regular dies. Characterization studies of this ribbon are now no longer impeded or complicated by unknown effects arising from the presence of SiC on the one face at least. The second significant consequence is associated with the increase in solar cell performance. This, by itself, is perhaps not as important in these preliminary experiments as the accompanying increase in material homogeneity relative to earlier levels, as evidenced by a tighter spread in solar cell parameters. Some results from displaced dies are given in Table II. The value of experiments designed to examine the influence of growth parameters and cartridge design changes on material quality often had been negated in the past by material inhomogeneity. This situation should be much improved at the present level of cell performance.

A number of interesting features in the data of Table II are worth pointing out. In spite of the limited statistics, these are consistent with information obtained from runs not using deliberately displaced dies in most instances, and are not intended to necessarily represent evidence for material changes arising from the displacement-induced asymmetry itself:

(i) Possible reasons for the striking difference in electrical properties obtained for cells made from the two ribbon faces (run 18-96) are examined in Section IV. At present there is not sufficient data to link this difference to specific growth condition changes arising from die asymmetry. However, it was reproduced in all the displaced die runs over the range of growth conditions covered. The growth speed of the ribbon varied from 2.3 to 3.8 cm/min except as noted in Table II. It is worth repeating at this time that it appears, in retrospect, that die top conditions equivalent to those achieved deliberately by die flat displacements were likely realized by accident in earlier runs as a result of non-uniformly machined die tops (such as the documented case of run 16-090). This could consequently also give rise to some of the material inhomogeneity characteristically observed in ribbon grown from nondisplaced dies.

(ii) Some effects of growth speed on material quality have been observed. The net impact of speed on solar cell performance cannot be evaluated on the basis of the available data.

(iii) The optimum cell performance to date has been achieved with a central capillary die and 0.050 cm wide top slot, run 18-102. Growth

speeds in this run were in the lower range explored, between 2.3 and 3.0 cm/min.

(iv) Average parameters in a given run for cells made from ribbon cut as 2.5 cm by 7.5 cm strips with the longer dimension sampling the full width of the ribbon usually are higher and show less scatter than those for narrower ribbon grown from above the capillary exit region.

Additional data, in the form of IR photoresponse scans on solar cells, spreading resistance measurements, and cross-section examination are needed to help in the identification of melt impurity transport processes which could be responsible for producing the trends in the results obtained to date. Theoretical considerations have shown that the extreme aspect ratio of the ribbon (width much greater than thickness) favors melt impurity transport to be diffusion controlled across the ribbon thickness, but convection dominated over distances of the order of the ribbon width.[2] The data will be examined with a view toward attempting to determine whether this may be a reasonable assumption for the growth conditions encountered here.

Examples of IR scan spectra representative of ribbon solar cells made from material grown from central capillary dies for a variety of growth conditions are shown in Figs. 3 to 6. The scan in Fig. 3(a) is made across the ribbon width of a narrow (~4 cm wide) ribbon grown from above the capillary exit in a central five-capillary die at a speed of 3.4 cm/min. The envelope through the peak response points has been interpreted as reflecting convective redistribution across the ribbon width. According to the model for this redistribution,[2] the concentration of low segregation coefficient ($k_o \lesssim 10^{-2}$) and high liquid diffusion coefficient ($D \gtrsim 10^{-4}$ cm^2/sec) impurities will be depleted in regions above the capillary exits and enhanced farthest downstream from them (here the ribbon edge). If impurities detrimental to solar cell performance were to be redistributed by this mechanism, the shape of the cell response spectra would be expected to reflect this in a manner similar to that observed. Comparable results have been reported earlier[3] and are also observed in Figs. 4(a) and 6.

Significant deviations from the peak response envelope are observed regularly in the form of sharp dips in the cell spectra, representing areas of the cell very poor in comparison to the regions of peak performance. The cause for this deterioration is not known and cannot be deduced on the basis of these scans alone. Some insight into possible

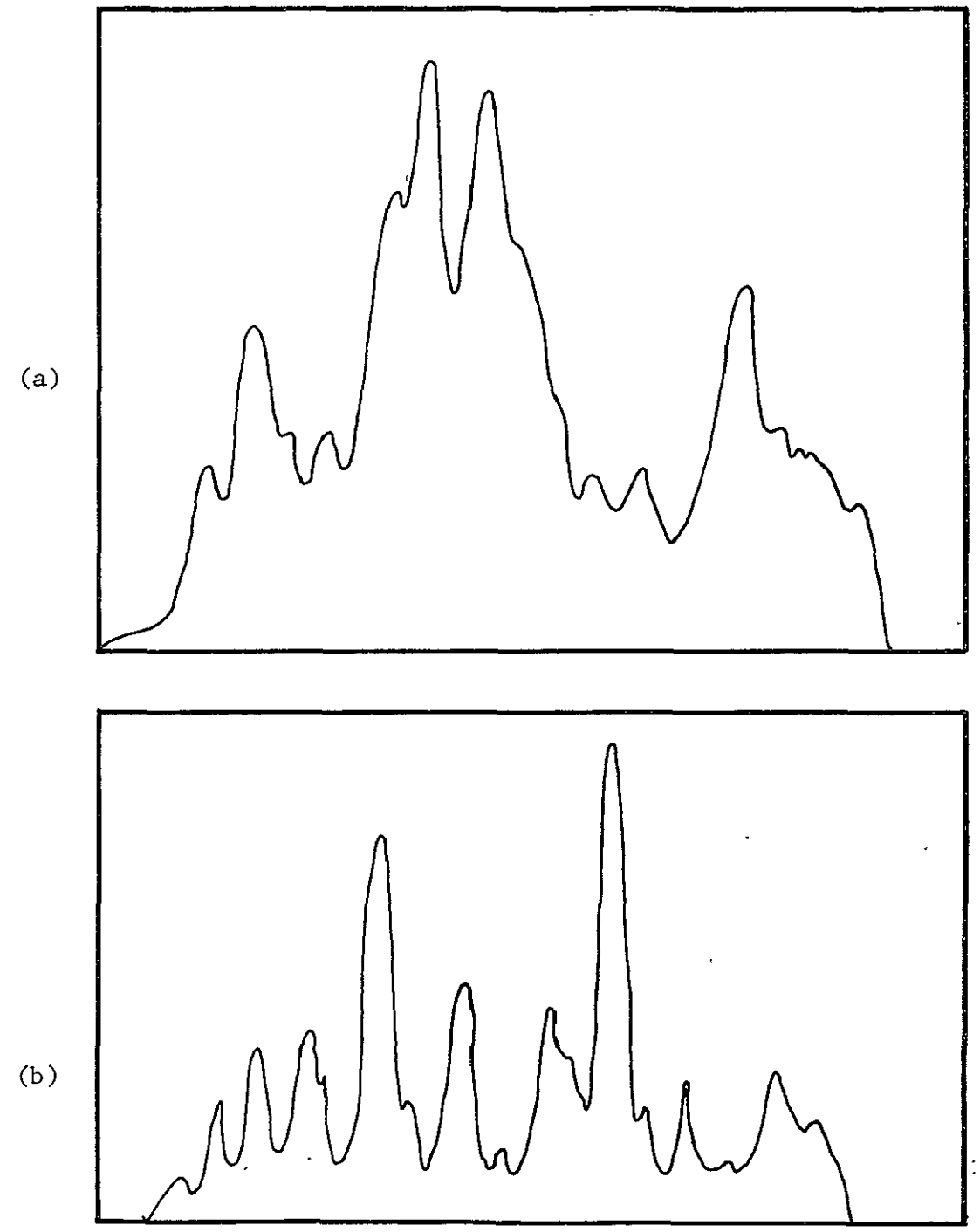

Fig. 3. IR scans across solar cells made from narrow (~4 cm wide) ribbon grown from directly above the capillaries in central capillary die in run 18-73. Scans are taken transverse to growth direction. Growth speeds are (a) 3.4 cm/min, and (b) 4.6 cm/min.

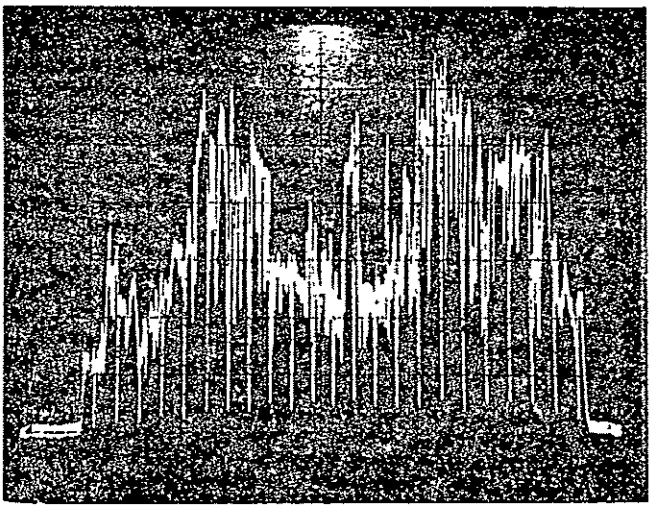

Distance across cell →
(a)

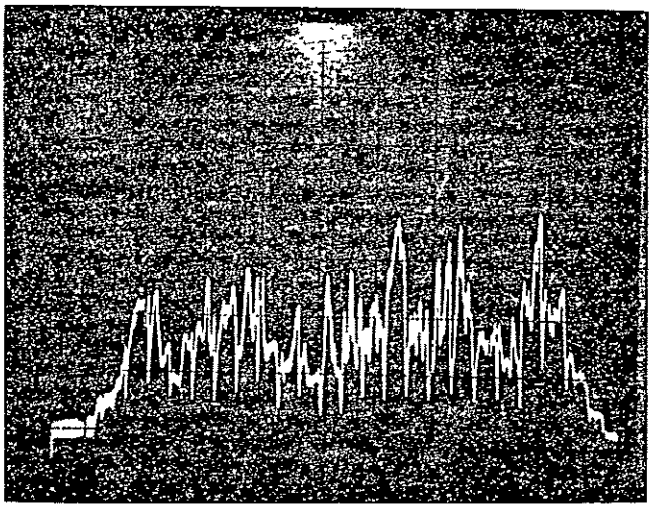

Distance across cell →
(b)

Fig. 4. IR scans of solar cells 18-102-12 and 18-102-8 (see also Table II) made from ribbon grown from a central capillary die in run 18-102. Scans are taken across nearly the full width of the ribbon, perpendicular to the growth direction at growth speeds of (a) 2.3 cm/min, and (b) 3.1 cm/min. The regularly spaced signal minima reflect positions of grid lines crossed in the scan.

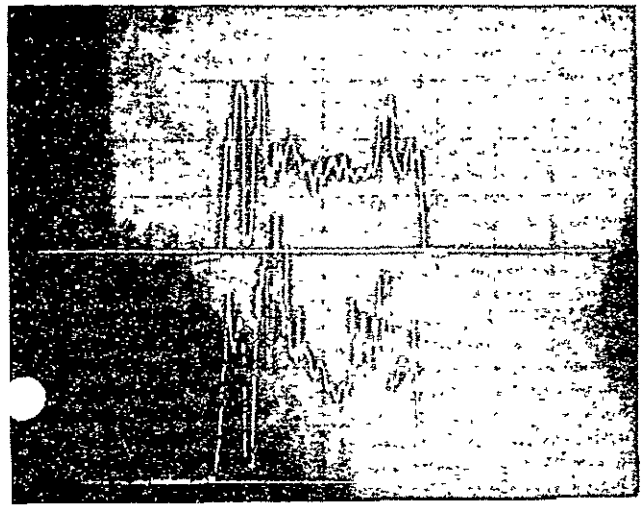

(a)

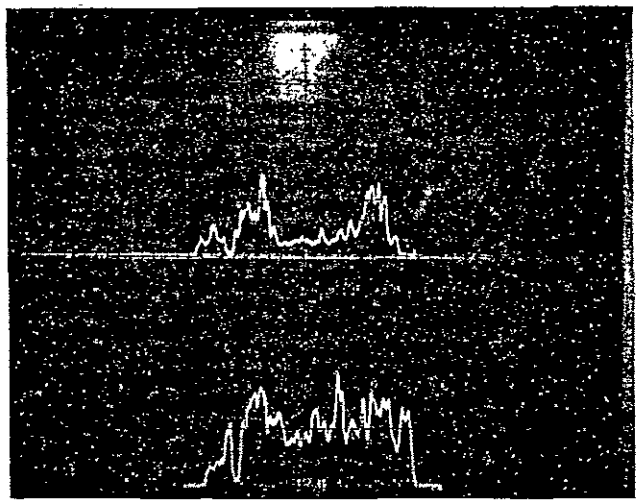

(b)

Fig. 5. IR scans of solar cells 18-97-6 and 18-97-9 (see also Table II) made from narrow (~4 cm wide) ribbon grown from directly above the capillaries in central capillary die in run 18-97. Scans are taken transverse to the growth direction at growth speeds of (a) 3.3 cm/min, and (b) 4.5 cm/min.

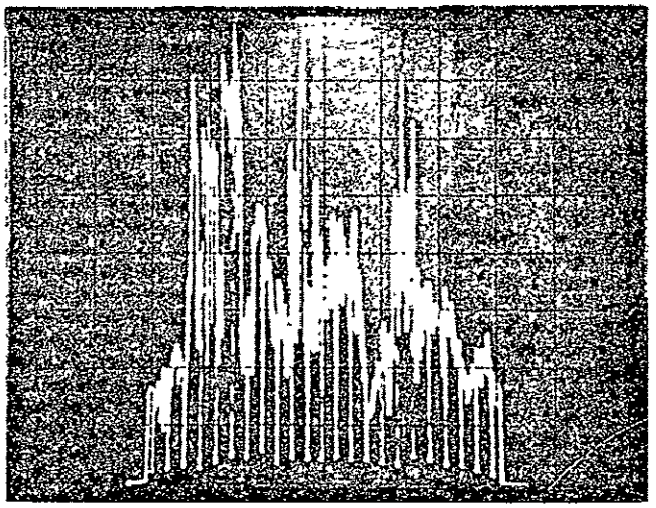

Distance across cell →

Fig. 6. IR scan of solar cell made from ribbon grown from central saw cut die in run 18-90 at a speed of 3.5 cm/min. Scan is taken across nearly the full width of the ribbon. The regularly spaced signal minima reflect positions of grid lines crossed in the scan.

origins of the larger regions of poor response, such as that occurring in the central part of the spectra in Fig. 4(a), comes from observing the changes in response incurred with an increase in speed. For examples of this, compare the scans for different growth speeds in each of Figs. 3, 4 and 5. The central degradation of cell performance often appears to become so severe at the higher speed as to dominate the response and overwhelm the normal features (as in Fig. 3(b)). The change in speed was incurred in all cases, while continuing growth of the same ribbon without interruption. To maintain constant width growth, some changes in die top isotherm shape were necessitated, however. These generally resulted in growth of thinner ribbon at the higher speed.

Reflections on possible causes of the IR scan spectra variations described lead to the realization that the interface growth phenomena which are likely to be responsible involve interactions of convective and diffusive melt impurity transport with effects due to ribbon thickness and interface shape variations. In the modeling of impurity transport which has predicted convective redistribution across the ribbon width, such interactions are not included. Planar growth interfaces and uniform ribbon thickness are assumed, and melt flow is taken to be laminar. The experimental data gathered to date can be interpreted to signify that deviations from these idealized conditions are very much to be expected and become greater as the growth speed increases for the die designs used. Nevertheless, the model for impurity transport can be utilized to provide valuable guidance toward improving the ribbon growth process in order to optimize material quality.

The IR scan spectra also can be used to illustrate the desirability of adopting standardized sampling of ribbon material in order to judge levels of quality and solar cell performance in the case of growth of wide ribbon. Because of the irregularity in the response curve typified by the spectra in Fig. 4(a), a significantly different measure of cell performance would be obtained if a sample which spanned the central 3 cm of the ribbon were considered rather than the full 7 cm width. On the other hand, the comparable difference in the case of the sample of Fig. 4 (b) may not be detectable. In another situation, the effect of speed on material quality would be more pronounced in the case of narrow ribbon growth (e.g., Figs. 3 and 5) than for wider ribbon. The entire change in performance levels of the material with speed would then be wrongly attributed to growth speed effects, rather than being recognized as arising partially from the sampling procedure. Furthermore, this sampling would

not reflect accurately the capability of the system to grow wide ribbon of a given level of performance. The inconsistencies that may arise are illustrated by the cell parameter values for both wide and narrow ribbon grown in runs 18-96 and 18-97 given in Table II. Again, even though the differences reflect real effects of changes in growth conditions on material quality, care has to be exercised as to which results are taken as a measure of the full capability of the system in producing wide ribbon of a given performance level.

Up to this point, only the causes for material inhomogeneity across the ribbon width have been examined in connection with expected convective impurity redistribution. As was noted above, the complexity of the data reflects the fact that processes related to changes in the ribbon thickness dimension cannot be ignored. Parameters related to the ribbon thickness and interface shape and irregularity now are shown to play an equally prominent part in melt impurity transport. Knowledge of the interface shape during EFG of ribbon is limited at this time, but some information is available from spreading resistance traces. An example of this is given in Figs. 7 and 8 for ribbon grown from a displaced die in run 18-90. The material was grown with a central saw cut die from an undoped melt in order to facilitate studies of residual impurity levels in the system. The first three traces (Fig. 7(I), (II), (III)) are taken across the full width of a 7 cm wide ribbon, perpendicular to the growth direction. The variations in resistivity are quite large and are very similar as a function of width both along the surface (Fig. 7(I)) and within the thickness cross-section (Figs. 7(II) and 7(III)). The average resistivity level over the central part of the ribbon is about 30 Ω-cm. Noticeable decreases occur toward the ribbon edge, where the resistivity drops to as low as 0.2 Ω-cm.

Traces showing the resistivity variation across the ribbon thickness are shown in Figs. 8(a) - 8(g). Their different lengths reflect ribbon thickness variations arising from the intersection of a beveled surface of constant angle and the ribbon. The approximate location of each trace in Fig. 8 with respect to the ribbon width is marked in Fig. 7. All traces go from the ribbon face grown above the low meniscus side on the left, to the high meniscus side ribbon face on the right. Two features stand out in the majority of the thickness traces: a rather sharp, almost discontinuous increase in resistivity not far from the low meniscus side ribbon surface, and a more gentle resistivity minimum located generally nearer the high meniscus side ribbon surface. On the average,

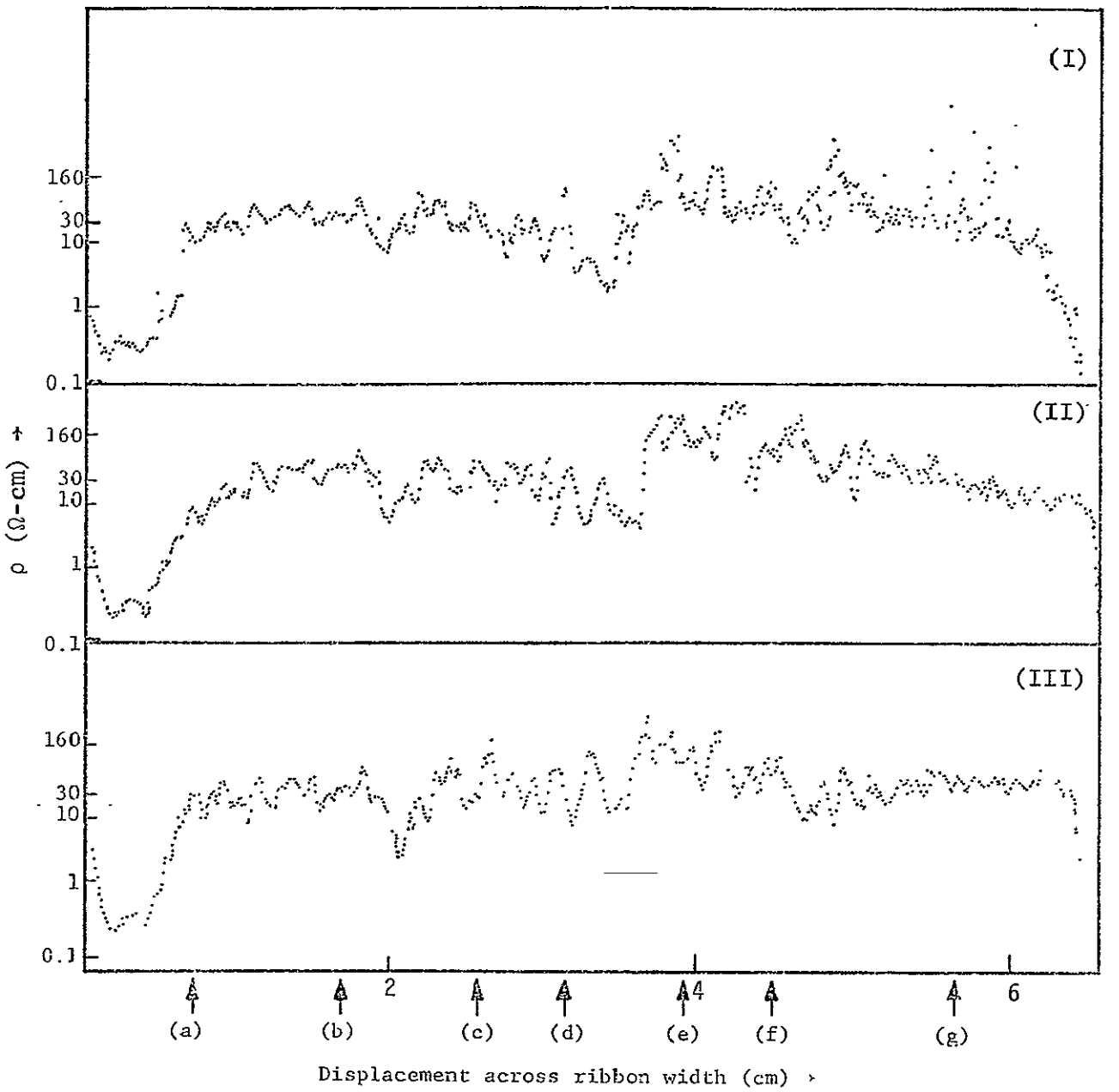

Fig. 7. Spreading resistance data from displaced die run 18-90. Traces are taken transverse to the growth direction and span the full width of the ribbon: (I) on the surface grown from above the low meniscus side of the die; (II) and (III) within the ribbon cross-section. Arrows indicate positions of cross-section trace data reported in Fig. 8.

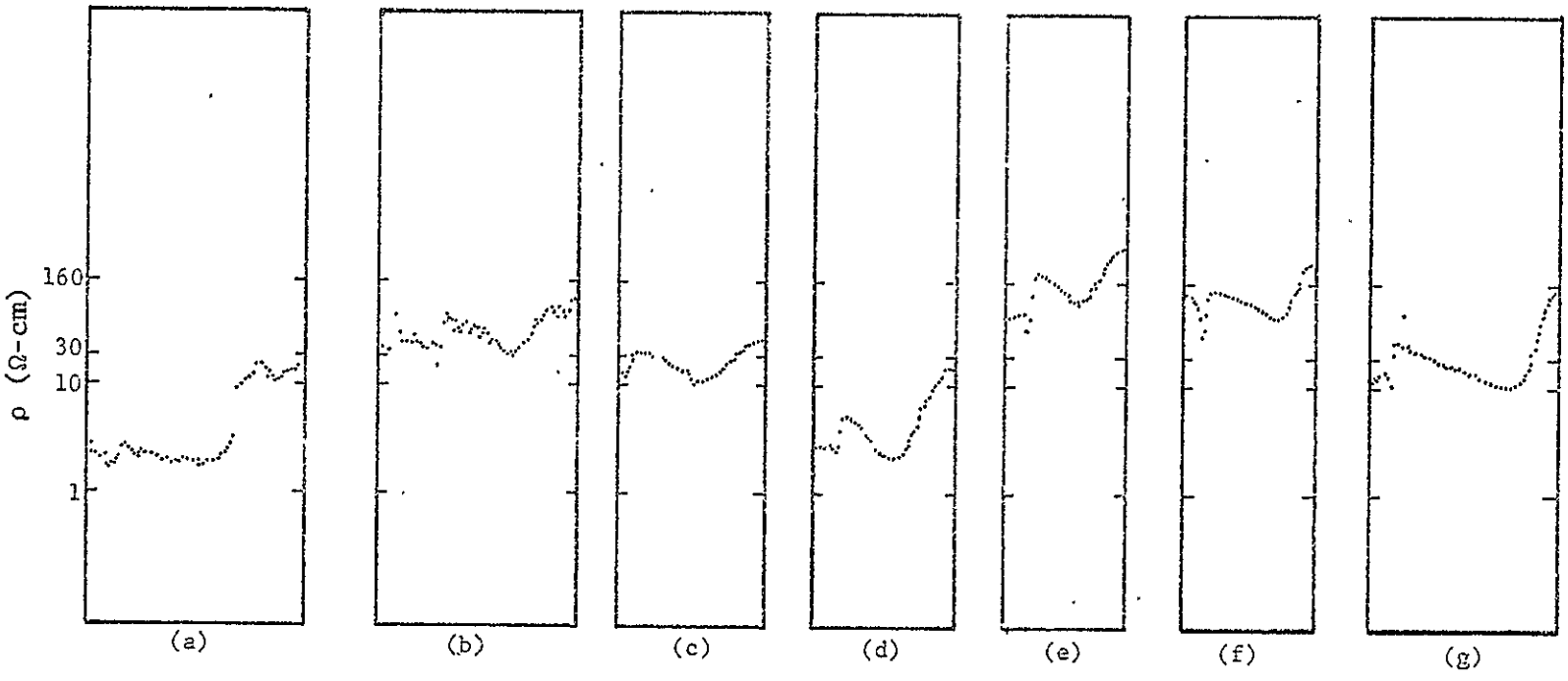

Fig. 8. Spreading resistance data from displaced die run 18-90. Traces are taken on a beveled surface within the cross-section of the ribbon at locations indicated in Fig. 7. The traces go from the low meniscus surface on the left to the high meniscus surface on the right.

the discontinuity is located about 50 μm from the low meniscus surface, while the resistivity minimum is about 100 to 150 μm from the high meniscus surface. It is also worth noting that the resistivity traces within the cross-section show considerably less scatter than those across the width, except for the neighborhood of the discontinuity.

The large decrease in the resistivity as the ribbon edge is approached shown in the traces in Fig. 7 reflects a variation in net carrier concentration of about two orders of magnitude, and indicates significant impurity redistribution is taking place within about 1 cm of the ribbon edge. The resistivity variations track the IR scans of Fig. 6 in their general features, with low values corresponding to poorer regions of the cell, and high values to the better cell areas. (The measurements in Figs. 6 and 7 were made on the same ribbon grown at a constant speed, but not on the same sample. Thus, a one-to-one correspondence is not possible.) Even though levels of specific impurities are not revealed by these measurements, the data suggest that the IR spectra variations are caused by fluctuations in impurity levels, some at least on the scale of the ribbon width. As noted earlier, convective impurity transport in the die top melt can account for such variations. However, care must be taken in applying this argument to the regions very near to the ribbon edges because this is also a place where the ribbon thickness changes very rapidly, often by a factor of two or more.[1]

The most notable aspect of the cross-sectional resistivity traces of Fig. 8 is the evidence they give of impurity redistribution mechanisms operative in the ribbon thickness dimension, which at the same time reflects a degree of growth system asymmetry. While mechanisms in the melt which could account for the features observed are not well understood, the data appear to be consistent with asymmetry observed in ribbon cross-section structure, to be discussed below.

Cross-sections of ribbon grown from displaced dies have been made, to look for structural changes that may arise from growth interface asymmetry introduced by the displacement. Representative cross-section photomicrographs are shown in Figs. 9 and 10. A recurring feature of ribbon grown from high speed cartridges in JPL No. 1 and No. 3A has been the presence of a subsurface grain boundary structure.[3] It occurs also over much of the ribbon cross-section in the case of samples examined from run 18-96, but is visibly displaced toward the low meniscus ribbon surface (high die side), as shown in Fig. 9. Because of a generally high level of SiC on this surface, which is known to depress solar cell

CELL NO. 968
η = 8.53%
JUNCTION SIDE UP
HIGH MENISCUS SIDE UP

$\bar{t}$ = 387 μm $\bar{x}$ = 243 μm

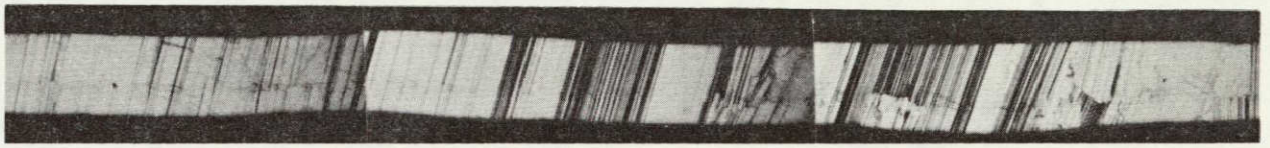

$\bar{t}$ = 376 μm $\bar{x}$ = 242 μm

CELL NO. 969
η = 3.75%
JUNCTION SIDE UP
HIGH MENISCUS SIDE DOWN

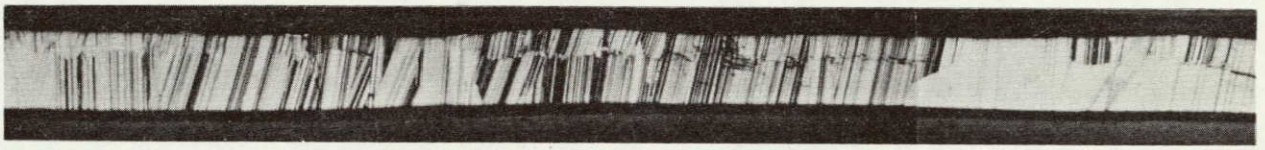

$\bar{t}$ = 349 μm $\bar{x}$ = 98 μm

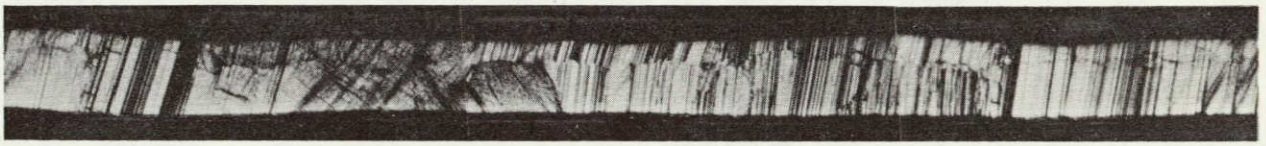

$\bar{t}$ = 342 μm $\bar{x}$ = 89 μm

250 μm

Fig. 9. Typical cross-sectional structure of solar cells grown from a displaced die configuration (run 18-96, displacement = .012 cm). Symbol $\bar{t}$ denotes average ribbon thickness and $\bar{x}$ the average displacement of the cross-sectional structure from the junction face.

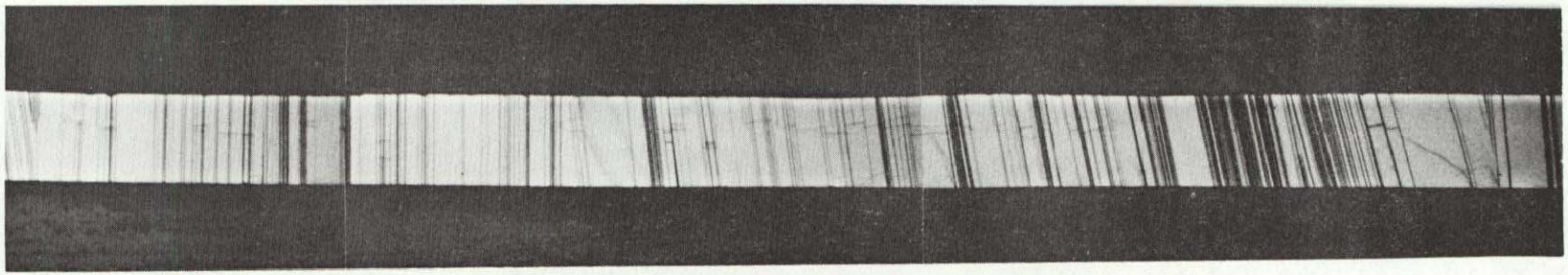

Fig. 10. Typical cross-sectional appearance of material grown from displaced die configuration in run 18-90 at a speed of 3.5 cm/min. The low meniscus surface is at the top of the picture.

performance, it cannot be deduced from this data whether the presence of the cross-section grain structure also contributes to degrading the efficiency of cells made with the junction on the low meniscus side ribbon surface.

Evidence for the formation and displacement of a cross-sectional grain structure in the ribbon grown in run 18-90 is not as strong; a representative cross-section photomicrograph is shown in Fig. 10. Two unusual features indicate the probability that conditions for the formation of cross-sectional structure were only marginal. The first is the presence of what appear to be discontinuous segments of grain boundaries extending parallel to the surface, as shown in Fig. 10. These are predominantly found near the ribbon surface growing from above the low meniscus side. In addition, high density clusters of dislocations appear sometimes in bands, usually in the half of the ribbon cross-section closer to the high meniscus ribbon face. The relation of these features in the cross-sectional structure to the resistivity variations found across the ribbon thickness (Fig. 8) is not known. However, it is likely they both reflect changes in interface shape resulting from deliberately created asymmetry arising from the use of displaced dies. Possible mechanisms which could result in the formation of central grain structure and its implications in impurity redistribution have been discussed in an earlier report.[3]

3. Future Work

The preliminary experiments with displaced dies have demonstrated that the imposition of asymmetric growth conditions with respect to the ribbon thickness dimension can have potentially beneficial consequences for material quality and solar cell performance. The data suggest that the interface phenomena associated with impurity redistribution effects, which could be responsible for material improvement, are very complex. One aim of future work will be to study the effect of certain changes in growth conditions on material quality in search for the most important factors contributing to the improvement of quality.

One area which will continue to be emphasized will be that of die design. Although the central capillary die has produced the best material to date, it nevertheless appears to suffer from several potentially serious disadvantages. The growth of SiC in critical regions of the capillaries appears to be undesirable both from the point of view of growth reliability and material quality. The localized heating of the

central portion of the ribbon is observed to lead to thinning of the ribbon, an effect which becomes more pronounced as the growth speed is increased. The effects of this on material quality are not known, but it can be conjectured that regions of poor solar cell performance in the central part of the ribbon, such as that shown in Fig. 4(a), are associated with non-ideal melt flow conditions occurring at the capillary exit. These conditions could be expected to become more deleterious to material quality with growth speed increases, as is observed, since the potential for melt flow irregularities and turbulence increases. A reasonable alternative to the central capillary arrangement appears to be the central saw cut die. This distributes the melt flow over a larger cross-sectional area, while at the same time providing the opportunity to constrict the flow so as to take advantage of possible convective redistribution of impurities to the ribbon edges.

Theoretical and experimental examination of the effect of interface shape changes on material quality will also be undertaken to attempt to understand the influence of interface shape on material quality. In this connection, displaced die experiments will be continued to explore the limits of stable growth conditions available with both die and cartridge system component asymmetries.

III. MULTIPLE RIBBON FURNACE by B.H. Mackintosh

A. Background and Progress Through January 1978

Mobil Tyco began the development of a technology for high productivity manufacture of silicon ribbon in 1975. This technology, based on modular design of crystal growth apparatus and on operation of multiple growth units in large furnaces, is embodied in the equipment known as Furnace 3A operated under this contract. Funding by JPL of development work on this equipment began in February 1977. Growth of 5 cm wide ribbon had first been accomplished shortly prior to that date. It was the overall goal of contract year 1977 to demonstrate that five ribbons of 5 cm width could be simultaneously grown by one operator at a 7.5 cm/minute rate. Subsidiary tasks for the year included the design of a method for continuous melt replenishment and development of automatic growth control via optical sensing of ribbon width. The feasibility of multiple ribbon growth was demonstrated in principle in January 1978. The main shortfall of contract year 1977 was that the growth rate goal of 7.5 cm/min was not achieved; the standard growth setups produced ribbon of good mechanical quality only at 3.5 cm/min. Yields of full-width ribbon and duty rates for growth were also low. Furthermore, this multiple growth system was not capable of operating in a clean mode, and therefore its output material was not made into solar cells.

A significant event of 1977 was the use of SAMICS to project the cost of large scale manufacturing of silicon ribbons by EFG. It was shown that a scaled-up version of the present Mobil Tyco multiple furnace producing ten ribbons 7.5 cm wide at 7.5 cm/min per operator at 90% yield and 83% duty rate would manufacture cell blanks at $\$11.80/m^2$ value-added cost.[4]

Taking into consideration the promising nature of this approach to high-productivity silicon sheet production, three tasks were defined for

the present multiple growth system for the 1978 contract year. The first task was to demonstrate that a furnace of this size and complexity could produce ribbon of suitable quality for solar cells. The second task was to develop the various subsystems so that the overall system would perform with duty rates and yields approaching levels required in a manufacturing situation. The third task was to further evaluate the "high speed" growth cartridge which had been designed and built but not thoroughly evaluated in 1977. A plan was established to demonstrate, by the end of 1978, operation of the furnace at 70% duty rate, and a 70% yield of material producing 9% or better solar cells. The other two furnaces operated under this contract, System 1 and System 17 (built during 1978) were expected to generate information which would contribute to attainment of these goals.

B. Progress on Ribbon Quality Subtask Through June 1978

The condition of Furnace 3A at year's beginning was such that the melts were almost certain to be contaminated with metal particles from the stainless steel hot zone shell, trap doors, and cartridge side walls. The major element of the clean-up program was thus to redesign these components using more appropriate materials and construction methods. A prototype for a suitably cleaned-up furnace hot zone had been designed and partially constructed in 1977. This unit, designed for operation of two growth cartridges, or one growth cartridge plus the melt replenishment cartridge, was completed and tested in March 1978. Cartridges were redesigned to eliminate stainless steel parts, and the trap doors were removed. A series of highly standardized single-ribbon runs from non-replenished melts was then undertaken to evaluate the effectiveness of these clean-up measures. A severe, unexpected problem was encountered with silicon carbide particles. Very little full-width ribbon could be grown and freezes were frequent. Solar cells made from this material displayed low open circuit voltages and fill factors attributable to junction shunting (Table III). However, two positive results were obtained from these runs. Analysis of the silicon by emission spectroscopy revealed that previous high concentrations of metallic impurities had been reduced to the range of 5 to 10 ppm, a level similar to that seen in material from Furnace No. 1 which had been in a deliberately clean mode of operation for several months. The other positive result was seen when the characteristics of solar cells grown from quartz crucibles in this series of runs in Furnace 3A were compared with those of cells made from

Table III. First Series of Baseline Quality Runs. Averaged Solar Cell Characteristics for Ribbons Grown from Furnace 3A after Standard Processes. 100 mW/cm^2. 28°C. No AR Coating.

Run No.	No. of Cells	Area (cm^2)	J_{sc} (mA/cm^2)	V_{oc} (Volt)	FF	η (%)	L_n (Dark) (μm)
16-110	3	21.2	15.15	.403	.43	2.76	5.5 - 7.5
16-111	1	21.2	16.57	.304	.32	1.61	9 - 15
16-112	7	21.2	14.05	.398	.43	2.42	4 - 12
16-113	15	21.2	12.36	.478	.63	3.73	3 - 7
16-114	6	21.2	14.19	.369	.35	1.84	-
16-115	2	21.2	10.13	.275	.31	.88	-
16-116	8	21.2	11.87	.302	.33	1.22	2 - 3
16-118	6	21.2	16.53	.329	.35	1.93	7 - 14

Table IV. Photovoltaic Characteristics of Solar Cells after SiC Removal.

Run No.	Cell No.	Area (cm^2)	J_{sc} (mA/cm^2)	V_{oc} (Volt)	FF	η (%)
16-114	1A	10.9	14.33	.510	.729	5.33
	3B	9.44	14.83	.522	.678	5.25
	5A	4.90	14.50	.506	.681	5.0
16-116	1B	1.18	13.21	.493	.691	4.50
	3B	4.05	12.86	.482	.629	3.90
16-118*	2A	2.20	14.36	.524	.725	5.46
	2B	2.16	15.0	.528	.754	5.97
	2C	1.87	15.83	.532	.749	6.31
	4A	3.30	16.85	.533	.712	6.39
	7A	5.94	17.17	.532	.680	6.21
	7B	3.30	17.45	.526	.584	5.36

*Quartz crucible run; others graphite.

graphite crucible material. This comparison, made on small areas of cells chosen to be free of silicon carbide, showed the photovoltaic characteristics of quartz crucible grown material to be better than the graphite-grown material and, indeed, close to the 9% AM1 performance level required by year's end (see Table IV). (The same phenomenon of superior electrical parameters from quartz-grown material was seen in material produced by other systems at Mobil Tyco and has been under investigation internally.)

While the material grown in this series of quality-baseline runs was being analyzed, other work related to productivity (e.g., improvement of temperature control and puller subsystems) and to high speed growth was undertaken. Although we continued to experience poor growth stability and unusually high densities of silicon carbide particles, the causes of these difficulties were obscured by somewhat incidental factors. Operation of the cartridge off-center in the short hot zone caused lateral temperature gradients which could not be completely corrected with cartridge heaters. A batch of graphite crucibles, which were to be a standard component of all single-cartridge runs of the year, was found to be defective. The quartz crucibles temporarily substituted caused the familiar problem of deposition of silicon monoxide on cartridge components. Finally, the "high-speed" cartridge was investigated in six runs in May and June. Standard setup and operating data (position of heaters and heat removal element, gas flows, optimum growth rate, etc.) were not defined for this unit, and therefore stable growth was not expected to be achieved immediately.

At this time, experimental work on Furnace 1 generated important insights into the growth stability/silicon carbide problems of Furnace 3A. There, an attempt was being made to introduce oxygen into the silicon to improve device characteristics by means other than containing the melt in a quartz crucible. The outcome of these experiments, which entailed adding oxygen to the cartridge gases, was a dramatic demonstration of the effect on growth stability of contaminant gases. As little as 0.02 percent of oxygen in the helium introduced near the growth interface for cooling purposes disturbed the position stability of the ribbon edges. The effect was unmistakable, as Furnace 1 had been operating consistently with excellent stability for many previous runs. In these stable runs, the furnace was believed to be essentially free of oxygen; graphite crucibles were used, and the large areas of hot molybdenum presented by the heat shields in the furnace effectively reacted with

residual oxygen. Other related experiments in Furnace 1 showed the formation of silicon carbide in the region of the interface to be related to the presence of reactive species in the furnace atmosphere, although the relationship was not so clear. Following these results, work on the high speed 5 cm growth cartridge was discontinued so that efforts could be directed to solution of the silicon carbide problem which was seen as the major obstacle to demonstrating good photovoltaic characteristics in large area devices.

C. Progress on Ribbon Quality Subtask in Third Quarter

To begin the period of renewed efforts on ribbon quality, several measures were taken to reduce the level of atmospheric contaminants in Furnace 3A. The trap door system, removed in March prior to the quality baseline runs, was re-installed and the practice was adopted of keeping the furnace out of contact with room atmosphere except during short reloading periods. Furnace seals and gas plumbing systems were checked for leaks. A new hot zone insulation block was made so that the cartridge would be centered in the hot zone. The atmosphere in the furnace was then analyzed during six runs by drawing a sample stream through a gas cell in an IR spectrophotometer. This technique immediately revealed that the customary flushing rate of argon through the furnace was insufficient to prevent back-streaming of air around the cartridge opening. When the argon purging flow rate was increased to three times its usual value, CO and CO_2 concentrations were reduced to below the detection limits of this measurement technique, and ribbon could be grown with greatly improved stability. Repeatedly it was seen that when the argon flow rate was turned down, meniscus stability deteriorated. Data on four runs made with high purge rates at the time show a great improvement in ease of growth compared to runs 16-110 through 16-118, none of which produced more than 20% full-width ribbon (see Table V).

It is evident from these data, however, that even when air is effectively kept out of the furnace, quartz crucibles (when used) constitute an oxygen source which adversely affects growth stability. The key factor here is the design of the furnace/cartridge combination which forces furnace gases to exit via the channel through which the ribbon is pulled. This fact has two consequences. The entire furnace atmosphere outflow stream sweeps the meniscus, bringing into contact with it all reactive species which may be in the furnace, and possibly inducing turbulence. Secondly, helium is introduced, in the 5 cm growth cartridge,

Table V. Ribbon Growth Runs in July with High Argon Purge Rates - Furnace 3A.

Run No.	Crucible Type	Total Length Grown (m)	Percent Full-Width
16-138	Graphite	9.9	81
16-139	Graphite	8.5	60
16-140	Quartz	7.0	50
16-142	Quartz	7.3	30

Table VI. Improvement of Solar Cell Characteristics of Furnace 3A Ribbon. All Cells Approximately 2.2 cm by 10 cm, not AR Coated.

Month	Run No.	Crucible Type	Die Type	No. of Cells	Average Parameters			
					V_{oc} (Volt)	I_{sc} (mA/cm^2)	FF	P (mW/cm^2)
April	16-112	Graphite	MC	7	.398	14.05	.43	2.42
July	16-138	Graphite	MC	6	.498	14.79	.59	4.3
October	16-155	Quartz	SC	3	.527	17.96	.66	6.27
October	16-157	Graphite	SC	8	.507	17.28	.65	5.72

Die types: MC = multicapillary; SC = saw cut.

See Fig. 2.

into the ribbon channel about 1.5 cm above the heat removal element. As the outflow rate of furnace gases up this channel is increased, the amount of helium reaching the area of the heat removal element decreases until, at the high purging flow rates employed in these runs, no helium is available to increase heat transfer from the ribbon, and growth speeds are lower than normal. This situation was remedied in runs 16-155, -156, and -157 by adding a substantial flow of argon to the cartridge helium supply and reducing the main furnace purging flow, in addition to providing for it an alternative exit path. Under these conditions, the clean argon flow into the cartridge blankets the meniscus and carries the small quantity of helium to the heat-loss region where its presence is desired. An argon flow rate of 4.5 ℓ/min was used, in addition to the usual 0.7 ℓ/min of helium.

Growth stability was excellent and essentially unchanged when switching from graphite to quartz crucibles, suggesting that the meniscus was effectively being shielded from furnace atmosphere.

Solar cell characteristics have responded favorably to these efforts. Table VI presents comparative data for runs 16-112 (initial quality baseline run series in April), 16-138 (high purge rate, mid-July), 16-155 and 16-157 (first week of October, added argon flow to cartridge*).

The stable growth in run 16-155 of low-carbide ribbon from a quartz crucible may represent a breakthrough made possible by the technique of cartridge gas flushing. This will be true to the extent that the superiority of characteristics of devices made from quartz-grown material is due to a factor (e.g., a melt saturated with oxygen) which cannot practically be obtained in another way.

Some results of the important work done on Furnace 1 with die design were applied to Furnace 3A during the third quarter. The general intent of this work is to try to accommodate the impurities which may inevitably be present in EFG melts by concentrating them in a region away from the solar cell junction, or in a portion of the ribbon which can be removed in the course of device fabrication. The standard die used by Furnace 3A to grow 5 cm wide ribbon for over a year has been a multicapillary (drilled holes) type with a top slot .025 cm wide. In the last five runs of this reporting period, a "saw cut" capillary die with a .038 cm wide

*See discussion below of various die configurations used during this period.

slot was used (see Fig. 2, Section II). The central passage for feeding silicon up the die provides a degree of redistribution of impurities to the ribbon edges. This capillary configuration incidentally also contributes to easier growth control during spreading, as the small hot spots generated by silicon exiting from the drilled capillaries of the standard die are absent. It is apparent that solar cells made from ribbon grown using the saw cut capillary dies in Furnace 3A are better than "standard die" cells (see Table VII). However, it was reported in the July Monthly Report that cells made from ribbon grown in the 7.5 cm system (Furnace 1) using this type of die were not significantly better than those from multicapillary die material. This discrepancy is probably due to the fact that the solar cells made from 7.5 cm ribbon were cut so as to encompass the full width of the ribbon, whereas cells made from 5 cm ribbon were cut to 2.5 x 10 cm size by trimming off 1.25 cm from each edge of the as-grown ribbon. Thus, the 7.5 cm cells included both dirty and clean portions, while the cells from 5 cm ribbon were made of the clean portion only.

A die design which is probably more significant in the long run is discussed in Section II. This is the asymmetric-interface die in which impurities tend to segregate toward one face of the ribbon. Dies of this type are being made for Furnace 3A and will be evaluated in October and November. Beneficial results similar to those reported for 7.5 cm ribbon are expected.

Design work was begun on the new full-length hot zone in July. In addition to the requirement for cleanliness, design criteria for it were: (1) greatly improved mechanical stability, (2) better longitudinal temperature distribution, (3) more cost effective insulation material, and (4) convenience of servicing. When the relationship between atmospheric contaminants and growth stability became apparent, features were also added to reduce this contamination. This hot zone, for which parts are currently being made, is shown in Fig. 11. Principal features are as follows: insulation material is rigid fibrous graphite; the insulation pieces are machined from rectangular blocks. The insulation is made in four quarters sized to fit the large, high temperature halogen purification furnace which recently became operational at Mobil Tyco. All parts are mounted to two water-cooled structural members, a base plate and a top frame. This feature will eliminate the major changes in alignment among parts which occurred as the old hot zone was brought up to temperature. Three rectangular, slotted heating elements mounted on four graphite

Table VII. Comparison of Average Solar Cell Characteristics, Ribbon from Multicapillary vs. Saw Cut Capillary Dies. All Runs from Graphite Crucibles, all Cells Approximately 2.2 cm by 10 cm, not AR Coated.

Die Type	Run No.	No. of Cells	Average Parameters			
			V_{oc} (Volt)	I_{sc} (mA/cm^2)	FF	P (mW/cm^2)
MC	16-146	7	.486	15.94	.507	4.00
	16-151	10	.482	15.17	.543	4.03
	16-152	12	.494	16.00	.533	4.23
	AVERAGE	(Total 29)	.488	15.70	.530	4.11
SC	16-153	5	.515	16.94	.606	5.31
	16-154	4	.522	17.12	.640	5.74
	16-157	8	.507	17.28	.653	5.72
	AVERAGE	(Total 17)	.513	17.14	.636	5.60

Table VIII. Improvement of Growth Stability in 1978, Furnace 3A.

No. of Runs	Period	Percent of Ribbon Grown Full Width (> 4.5 cm)	Average Distance Between Freezes (m)
1*	January	45	.59
5**	July/August	56	1.41
5**	September/October	85	7.32

* Three cartridge run.
**Single cartridge run.

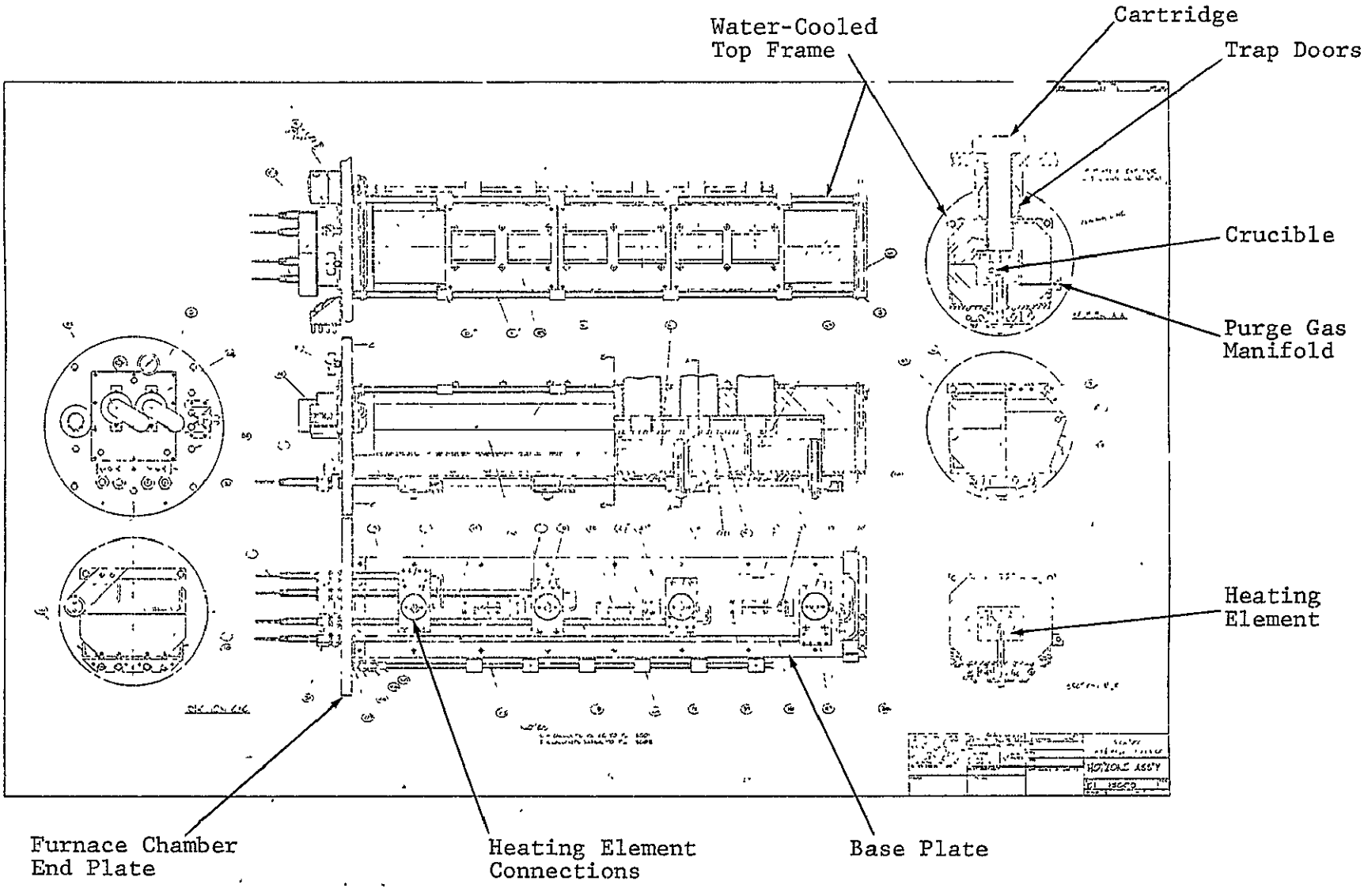

Fig. 11. New Hot Zone Assembly for Furnace 3A.

posts will be used. A family of heating elements has been designed which will provide various degrees of concentration of heating power toward the hot zone ends. By interchanging these heaters, a uniform temperature distribution may be quickly obtained. Connections to the heating elements will be made via a type of spring tensioned contact plate which has proven to be reliable in Furnace 17 and the short hot zone of 3A. A provision has been made for feeding part of the furnace purging argon flow into the interior of the hot zone. The cartridge will thus be in two concentric enclosures from which an outflow is maintained through relatively small openings. (The meniscus in each cartridge will also be blanketed as described above.) A version of the all-graphite quarter turn "trap doors" designed for Furnace 17 is being built for this furnace. The cartridges will be provided with gaskets to seal against the furnace top plate when fully inserted, and the openings in this top plate will have graphite liners to prevent contact between the cartridge and metal surfaces as they are inserted.

Several modifications have been made to the melt replenishment system to decrease its contribution of impurities. Stainless steel parts were designed out and a gate valve was added to close off the main feeding tube to atmosphere during reloading. Assembly and test of these redesigned furnace subsystems near the end of November will signal the completion of a major part of the ribbon quality subtask. Multiple growth demonstration runs will then be conducted.

The performance levels of solar cells made in recent single-cartridge runs show that the 9% AM1 efficiency figure promised for year's end is being approached. Long procurement delays for parts and materials, combined with time lost earlier in the year to various unforeseen problems, have placed the timetable for these demonstration runs about two months behind schedule. Thus, the final outcome of the year's work may not be demonstrated until January 1979.

D. Progress on Productivity Subtask

Operation of Furnace 3A in the five-ribbon mode in January 1978 served to demonstrate where efforts needed to be applied to increase the productivity of this system, i.e., number of square centimeters of ribbon of acceptable mechanical quality produced per operator hour. The greatest detractor of yield was the short average distance between freezes, or poor long-term growth stability. In addition, it was not generally possible to initiate growth from a full-width seed; spreading to full width

from narrow seeds was slow and precarious. Finally, the operator was required to perform some non-productive functions. Overall, progress has been made this year toward high-productivity multiple growth on two fronts. Many detailed refinements have been made to the temperature control and puller subsystems; these will be listed below. The more important achievement of the year, however, has been the identification of the relationship between the presence of reactive gases at the interface and unstable growth. At the start of 1978, it was believed that freezes might be a fundamental problem of silicon EFG, and a separate research task was created for the instrumented Furnace No. 17 to look into their causes. We have since then discovered that continuous growth for periods of many hours is possible when the growing ribbon is subjected to a sufficiently clean atmosphere. The principal mechanism by which frequent freezes and contaminated atmosphere are believed to be related is reduction of surface tension of the liquid silicon. With reduced surface tension, the meniscus at ribbon edges must be lower for ribbon edge position to be maintained. The size of fluctuations of die temperature and pulling speed which will be tolerated without causing a freeze is directly related to meniscus height. Thus, in general, factors which tend to increase meniscus height will improve growth stability.

In addition, the following design refinements made this year have contributed to or are expected to contribute to growth stability:

1. The drive system of the continuous pullers was redesigned to provide greater mechanical stiffness and to reduce periodic speed fluctuations.

2. A reduction in electrical noise picked up by the die temperature controllers is expected to result from certain design features of the new hot zone. The new main heaters will be electrically floating, permitting the choice of a grounding point which minimizes noise pickup. These heaters will be more rigidly mounted and more widely spaced from the thermal insulation, eliminating random arcing which was frequently encountered with the old hot zone. The control thermocouples will be thermally well shielded from convection currents and, hence, the output of the main power supply is expected to be more steady.

3. The cartridge afterheater systems have been equipped with closed-loop temperature controllers.

4. A die with wider overall tip dimension has been selected as the standard die for multiple growth. Preliminary work with these dies leads

to the impression that the higher meniscus and greater lateral thermal conduction of a wider die top promote growth stability. These advantages may, however, be sacrificed when an offset between the die tip levels is introduced to asymmetrically distribute impurities as discussed above.

A dramatic increase in growth stability has been demonstrated to result from the modifications implemented so far. Table VIII shows productivity-related information on runs performed at three periods in 1978. Although the figures in the first line are for a situation where three ribbons were being simultaneously controlled, these relatively low values are also typical of single-cartridge runs performed prior to the work outlined above. The other ten runs were single-cartridge non-replenished runs. Three runs of the last group of five were executed without a single freeze. (The quantity of silicon constituting the charge for a non-replenished run permits a maximum of 8 to 9 meters of ribbon to be grown.)

Several refinements have been made which will facilitate start-up of growth. Current limiters have been added to the cartridge power supplies so that full power can be applied to the cartridge heaters as soon as the cartridges are inserted. Further operator attention will not be required until the dies have filled and seeding can commence. The pullers have been outfitted with photo-electric sensors which will allow seed ribbons to automatically run down and stop within a short distance of the die. Circuitry has been provided to "ramp down" power to the end heaters simultaneously with ramping of the face heater set point. This provision has been found to facilitate full-width seeding.

These and other convenience features have been devised to help reach the goal of five ribbons, 5 cm wide, at 70% duty rate. Only the experience of operating this machine in full multiple mode will demonstrate whether or not one may realistically expect that a single operator could handle the ten 7.5 cm wide ribbons per machine, which has been the standard basis for price predictions, without more sophisticated automation features such as closed-loop control via optical sensing.

E. Progress on High Speed Growth Rate Task

A period of six weeks was allotted in the second quarter of this year for development of the growth cartridge designed in 1977 for growth of 5 cm wide ribbon at rates approaching 7.5 cm/min. Principal differences

between the growth system and the standard one are the temperature of the heat removal elements and the location of helium jets. Both these differences are intended to generate a steeper thermal gradient in the ribbon to promote growth at higher rates.

As discussed in Section III.B of this report, development work on this cartridge was hindered by extraneous factors, and we were unable to make substantial progress toward the growth of full-width ribbon at 7.5 cm/min within the allotted time period. In six of the ten growth attempts made, at least 1 m of ribbon was pulled. Maximum widths were 2.2 to 2.8 cm, and growth rates of up to 5.7 cm/min were observed. Growth stability was so poor and the tendency for the ribbon to spread so limited that the required remedies were not yet clear when this work was discontinued. Judging from the tendency of .03 cm thick by 5 cm wide ribbon to become buckled at rates over 3.2 cm/min, we expected that this high-speed growth task would evolve into an investigation of the cause of buckles as soon as meniscus stability permitting fast growth at full width was achieved. Questions of the relationship between growth rate (above the present level of 3 to 4 cm/min), ribbon structure, and electronic properties remain largely unanswered. Progress in EFG ribbon technology made this year by the three furnaces operated under this contract sets the stage for a highly productive year in which effort can be concentrated on these questions after the goals of the current contract year have been satisfied. Elements of the progress made this year which are particularly valuable in this regard are:

1. Identification of standard growth setups for 5 cm and 7.5 cm ribbon which will repeatably produce ribbon of known mechanical and electronic properties.

2. Resolution of serious problems with reliability of basic furnaces which slowed experimental work in 1977.

3. Construction of a new furnace, No. 17, with important new tools for research into silicon EFG.

4. Identification and control of factors affecting growth stability, greatly enhancing the ease of carrying out growth experiments, and improving the validity of experimental results.

IV. CELL CHARACTERIZATION by C.T. Ho

A. Overview

Ribbon material from both growth Stations No. 1 and No. 3A has shown considerable improvement in the photovoltaic properties during the last quarter. In the multiple growth system (Station No. 3A), the problem of forming high density SiC particles in the grown ribbons has finally been resolved (see Section III). Solar cells with conversion efficiencies in excess of 9% were produced in that furnace using the "short hot zone". In the wide ribbon growth system (Station No. 1), the major advance made was the use of displaced dies which resulted in gathering the SiC precipitates on one side of the ribbon surface. When the photovoltaic junctions were formed on the SiC-free surface, the variability of the cell parameters was greatly reduced, and larger batches of 2.5 cm by 7.5 cm cells (cut across the ribbon width) with average performances of over 9% resulted.

Photovoltaic properties of cells fabricated from material grown in graphite crucibles and quartz crucibles have been compared. In Furnace 3A, the ribbons grown from quartz crucibles on average yielded better photovoltaic performances. However, so far a similar comparison has been rather inconclusive for material grown from Furnace No. 1, perhaps because of evidence that the quartz used in the experiments might not have been of sufficiently high purity.

More studies are needed to understand the role of oxygen and particularly its interaction with other specific types of impurities which may in part limit the cell efficiencies to a plateau value of 9 to 10% at present. Further impurity analysis should be conducted in order to be able to identify the chemical nature of the impurities, their quantity and their distribution in the ribbon. The theory of fluid flow effects still needs to be completely confirmed experimentally.

B. Cell Evaluation for Growth Station No. 1

In Table IX we summarize the solar cell data for all the fabrication runs since our last quarterly report. For discussion, the results can be grouped as follows:

(i) Baseline Runs: Runs 18-78, -79, -83, -86, -92, and -100 are the routine growth runs for establishing the baseline growth conditions. All the runs were made using graphite crucibles and regular flat dies of various capillary configurations, such as multicapillary, central capillary, and central saw cut. The AM1 cell efficiency fluctuates between 7 to 8%, except in a later run, 18-100, which produced an average efficiency somewhat greater than 8%, demonstrating perhaps a general improvement in material quality which comes from standardizing routine procedures.

(ii) Quartz Crucible Runs: It is well known that oxygen in silicon can affect other electrically active metallic elements when they are simultaneously present. The classical example is Li in CZ growth silicon. Pell[5] reported how oxygen affects the nucleation of Li precipitates and diffusion rate of Li, and also how pair interaction leads to the formation of Li-O donor complexes. The possibility of interacting with Fe and other transition metals in silicon has also been suggested.[6]

In this program we have initiated a series of growth runs (18-80, -81, -82, and -85) in which we introduced oxygen by mixing about 1% by weight of crushed SiO_2 (quartz) powder into the silicon charge. The ribbons grown in these experiments show some quartz inclusions distributed non-uniformly near the edges on both surfaces. In the standard cell fabrication, highly leaky junctions were produced. We suspect that we may have unintentionally contaminated the quartz powder during the processes of crushing.

Run 18-88 was a growth run using a quartz crucible. Solar cells produced from this run have good junction characteristics, but low output. The diffusion lengths of the typical cells were 5 to 10 μm. In the next quarter, we intend to repeat the quartz crucible run with well-defined high quality crucibles, which are now being ordered, to exclude any suspicion that contamination of the melts with impurities from the quartz masked the effects of oxygen in these runs.

(iii) Displaced Die Experiments: The growth of ribbon by using a die with 3 to 5 mils of displacement at the die top has been described in detail in Section II. The most striking visible consequence arising is

Table IX. Summary of Solar Cell Evaluation Data for Ribbon Grown from System No. 1. ELH Light Source, 100 mW/cm^2, 28°C, Cell Area = 18 cm^2.

Run No.	Growth Parameter	No. of Cells	J_{sc} (mA/cm^2)	V_{oc} (Volt)	FF	η (%) No AR	η (%) AR Coated	Notes
18-78	Graphite Crucible Std CC Die	5	14.94	.506	.588	4.45	(6.45)*	CC = central capillary
18-79	Graphite Crucible Std CC Die	13	15.06	.514	.632	4.48	(7.08)*	
18-80 18-81 18-82 18-85	Crushed Quartz in Graphite Crucible	Junction Shunted						
18-83	Graphite Crucible Std MC Die	19	15.83	.506	.684	5.84	(7.95)*	MC = multicapillary
18-84	Graphite Crucible Std SC Die	43	15.32	.499	.646	4.95	(7.18)*	SC = saw cut
18-86	Graphite Crucible Std SC Die	9	15.27	.495	.689	5.21	(7.55)*	
18-88	Quartz Crucible Std SC Die	17	13.97	.475	571	3.82	(5.54)*	
18-90	Graphite Crucible Displaced SC Die (5 mils)	5	24.52	.473	.591		6.86	Undoped melt
18-92	Graphite Crucible Std MC Die	3	21.61	.520	.637		7.18	
18-95	Graphite Crucible Displaced SC Die (10 mils)	5	20.81	.522	.683		7.47	
18-96	Graphite Crucible Displaced SC Die (5 mils)	13(A) 4(B)	22.0 18.02	.523 .467	.712 .478		8.20 3.96	Surface "A" Surface "B"
18-97	Graphite Crucible Displaced CC Die (3 mils)	11	23.39	.529	.706		8.38	
18-100	Graphite Crucible Std CC Die	11	16.57	.528	.662	5.81	(8.42)*	
18-101	Graphite Crucible Displaced CC Die (3 mils)	7	22.6	.524	.684		8.12	Cell Area = 56 cm^2
18-102	Graphite Crucible Displaced CC Die (5 mils)	11	25.01	.540	.692		9.35	

*Numbers in parentheses are the projected values assuming 45% power gain on AR coating.

that the SiC particles are nearly all gathered at the low meniscus side of the ribbon surface, leaving the high meniscus side ribbon surface virtually free of SiC.

Runs 18-95, -96, and -97 were grown from displaced dies of various displacements. During the solar cell fabrication, the photovoltaic junction was made on the type "A" surface (containing no SiC), except for four cells from run 18-96, which were made on type "B" (containing SiC). In the latter case, the low conversion efficiency is believed to be mainly due to the junction shunting effect of the SiC. The SPV diffusion lengths measured on the cells from run 18-96 were found to be 20 to 22 μm for both types of surfaces. Thus, the displaced die growth appeared to have no first order influence on the bulk diffusion length of the grown ribbon.

Run 18-102, designed to provide optimum conditions in terms of die displacement and die design, indeed is an optimum run in terms of solar cell performance. The original measurement results on individual cells are reproduced in Table X. Notice that cell 102-11 with an area of 18.2 cm^2 has achieved a conversion efficiency greater than 10%. Further evaluation of cells from this run is underway.

C. Cell Evaluation for Growth Station No. 3A

Table XI summarizes the solar cell data for the material grown from the multiple growth system. The data may be discussed as follows:

(i) Establishing the Baseline Growth Condition: Most of the runs prior to 16-138 were designed to test the growth system. Runs 16-139 to -152 were devoted to resolving growth problems such as stability, freezes, and high SiC density (see Section III). Thus, the low cell performances in these runs reflect the difficulties encountered during the developmental efforts.

Run 16-148 is the beginning of a series of "quality status" runs after most of the system design and growth related problems have been resolved. Unfortunately, we did not obtain any information about the material quality between runs 16-148 to -152 because of several problems with the cell fabrication operation. Runs 16-153 and -154 were the final two baseline growth runs with graphite crucibles in the series. The cell baseline efficiency was then established as near 8%. This result is comparable to the baseline efficiency of Furnace No. 1 when the standard flat die is used.

Table X. Solar Cell Measurement Data for Run No. 18-102. ELH Light Source, 100 mW/cm^2, 28°C, AR Coated. All Cell Samples the Full 7.5 cm Width of the Ribbon.

Cell No.	Area (cm^2)	I_{rv} (mA/cm^2)	V_{oc} (V)	I_p (mA)	I_{sc} (mA/cm^2)	FF	P (mW/cm^2)
102-1	18.25	0.011	0.539	377.5	24.48	0.682	8.99
102-2	18.23	0.212	0.540	384.3	24.67	0.695	8.25
102-3	18.30	0.105	0.540	392.8	24.68	0.684	9.13
102-4	18.13	0.011	0.538	393.5	24.66	0.693	9.18
102-5	18.19	0.345	0.542	398.0	25.03	0.697	9.46
102-6	14.23	0.014	0.542	321.5	26.01	0.687	9.69
102-8	18.25	0.396	0.535	362.1	23.43	0.688	8.63
102-9	18.20	0.530	0.535	395.4	24.77	0.672	8.90
102-10	18.12	0.080	0.544	399.1	25.44	0.709	9.81
102-11	18.20	0.132	0.545	432.8	26.61	0.700	10.15
102-12	18.18	0.011	0.537	420.0	25.30	0.712	9.68
MEAN VALUE	17.84	0.168	0.540	388.8	25.01	0.692	9.35
STD ERROR OF MEAN		0.0545	0.0010		0.253	0.0036	0.136

Table XI. Summary of Solar Cell Evaluation Data for Ribbon Grown from System No. 3A. ELH Light Source, 100 mW/cm^2, 28°C, Cell Area = 21 cm^2.

Run No.	Growth Parameter	No. of Cells	J_{sc} (mA/cm^2)	V_{oc} (Volt)	FF	η (%) No AR	η (%) AR Coated
16-119		4	15.93	.485	.502	3.93	
16-135		2	13.53	.401	.439	2.49	
16-136		3	13.81	.397	.41	2.29	
16-137	Graphite Crucible Purge Rate Experiment	7	13.83	.503	.609	4.24	
16-138	Graphite Crucible Purge Rate Experiment	6	14.79	.498	.588	4.36	
16-139	Graphite Crucible Purge Rate Experiment	10	16.08	.491	.558	4.43	
16-140	Quartz Crucible Purge Rate Experiment	9	15.75	.436	.467	3.35	
16-141	Quartz Crucible Purge Rate Experiment	High SiC Density					
16-142	Quartz Crucible Purge Rate Experiment	9	14.22	.305	.342	1.53	
16-143	Graphite Crucible Purge Rate Experiment	10	15.28	.437	.419	2.83	
16-144	Graphite Crucible Purge Rate Experiment	12	15.07	.496	.563	4.20	
16-145	Graphite Crucible Purge Rate Experiment	18	14.43	.471	.507	3.52	
16-146	Graphite Crucible Purge Rate Experiment	11	15.80	.489	.517	4.03	
16-148 to 16-152	Graphite Crucible Baseline Runs	Fabrication Problem					
16-153	Graphite Crucible Std SC Die	5	16.94	.515	.606	5.31	(7.70)*
16-154	Graphite Crucible Std SC Die	4	17.12	.522	.640	5.74	(8.32)*
16-155	Quartz Crucible Std SC Die	3	17.96	.527	.663	6.27	(9.09)*
16-156	Quartz Crucible Std SC Die	6	17.36	.523	.662	6.02	(8.73)*

*Numbers in parentheses are the projected values assuming 45% power gain on AR coating.

SC = Saw cut die.

(ii) Quartz Crucible Experiment: After the completion of baseline runs with graphite crucibles, run 16-155 and -156 were the two following growth runs using quartz crucibles. The solar cells yielded an efficiency of about 9%. It is too early to speculate on the role of oxygen as an impurity in this experiment. More experimental runs are needed in order to decide whether the use of the quartz crucibles is more advantageous than using graphite crucibles as far as the photovoltaic properties are concerned.

V. MACHINE 17 by E. Sachs

A. Overview

The design and building of Machine 17 represented the single largest effort undertaken this year. Machine 17 was intended to be an instrumented crystal growth furnace for the investigation of some of the fundamental aspects of EFG growth. While the hardware that comprises the furnace itself represents several significant improvements and innovations over previous designs, the heart of Machine 17 lies in its instrumentation system. This instrumentation system is described in considerable detail in the text below. Also presented is the work done on growth system development, in particular, the mini cold shoe. Finally, some of the runs made to date on Machine 17 and their results are described along with the overall layout of the machine and the furnace construction.

B. Construction

Figure 12 presents a view of the entirety of Machine 17. The furnace stands at the center of the picture with the optical-video system in front of it. The rack panel to the left of the furnace houses power supplies and temperature controllers, while the rack panel further to the left houses the instrumentation panel and second TV camera. The desk to the right of the furnace holds the control panel, TV monitor and video tape desk.

Figure 13 shows a closeup of the slide-out hot zone. To date, this hot zone has been run in excess of 20 times without a single failure. This is an admirable reflection on its design. Its simplicity permits rapid changes to be made allowing large scale modifications of main zone temperature profiles.

One major innovation in furnace design introduced in Machine 17 is the use of cylindrical trap doors. The doors are sketched in Fig. 14 in position over the top of the hot zone insulation package. These trap

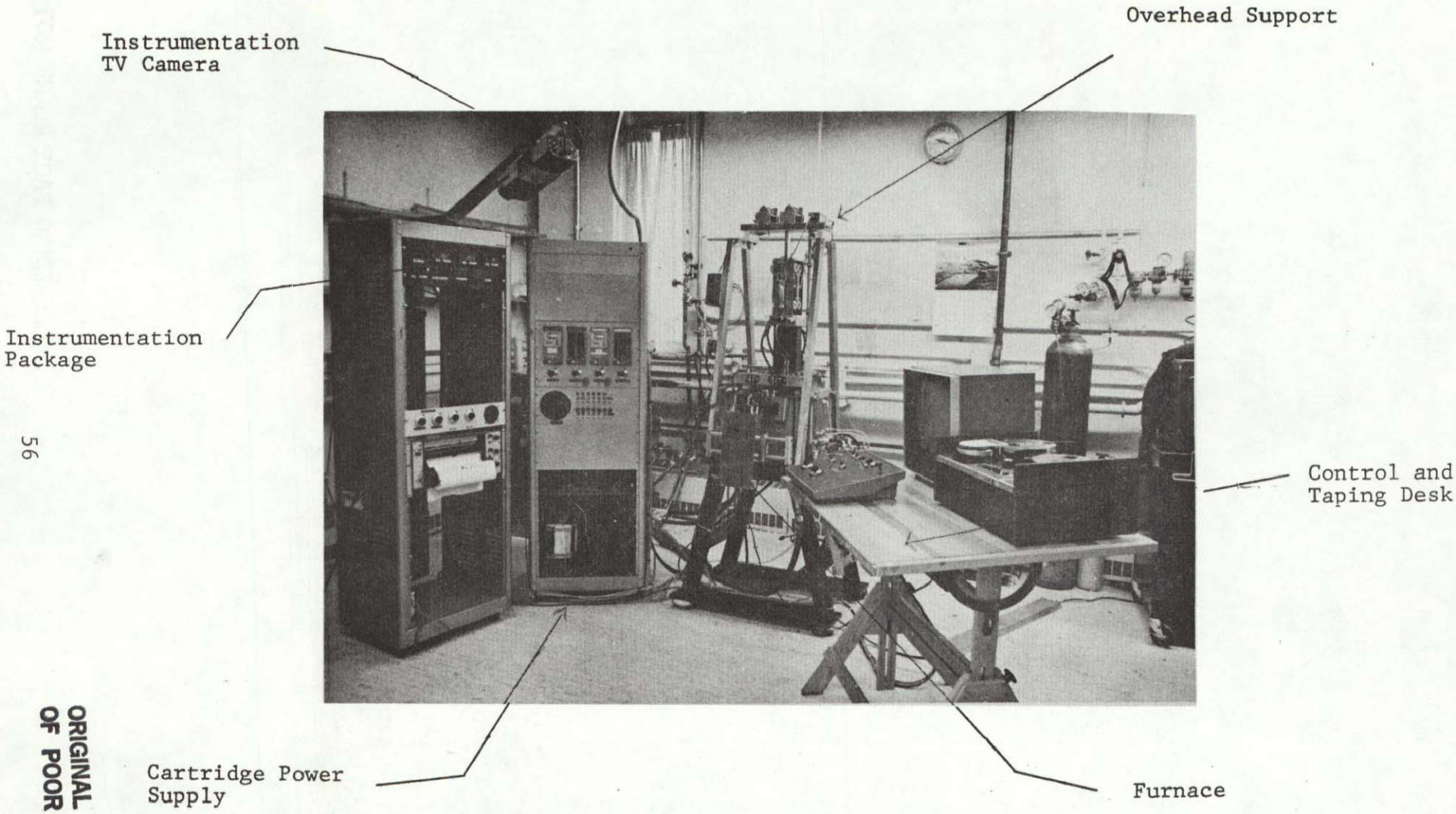

Fig. 12. Overall view of Furnace 17. Furnace is at center of picture with anamorphic optical system on front. The rack panel to the left of the furnace houses power supplies and temperature controllers, while the rack panel farthest to the left houses the instrumentation. The control and video taping desk is seen at the right.

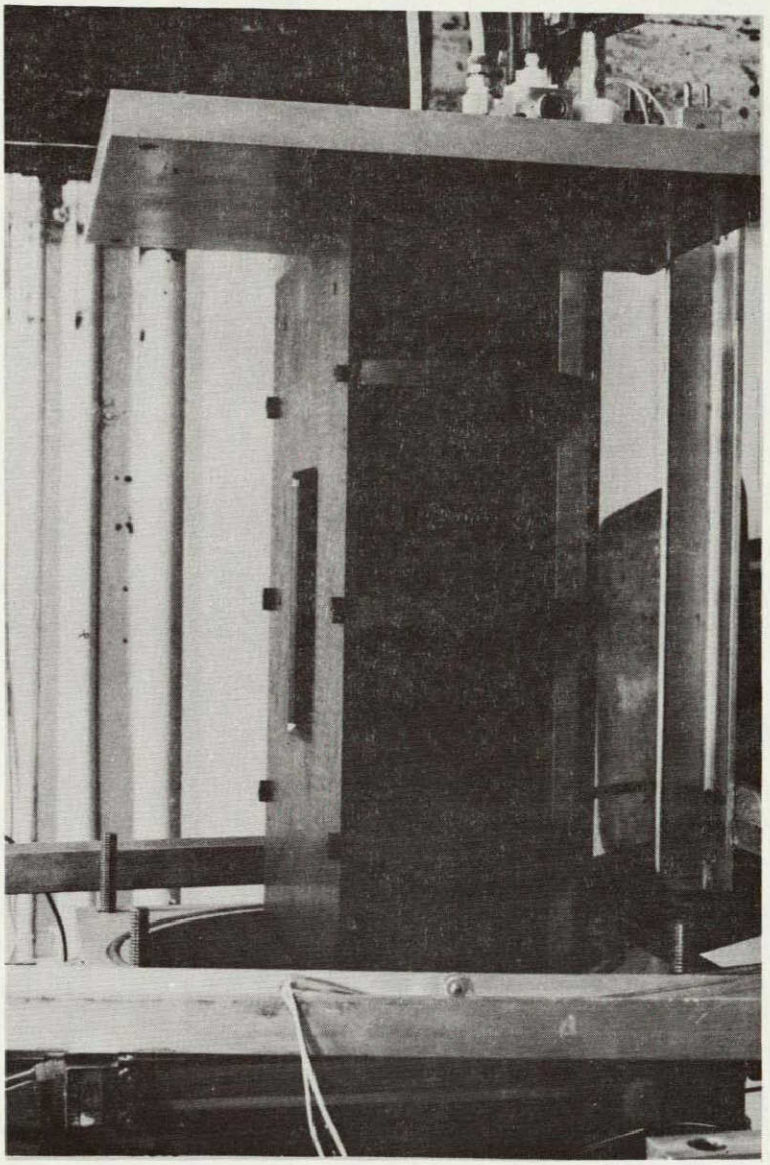

Fig. 13. Hot zone - Machine 17.

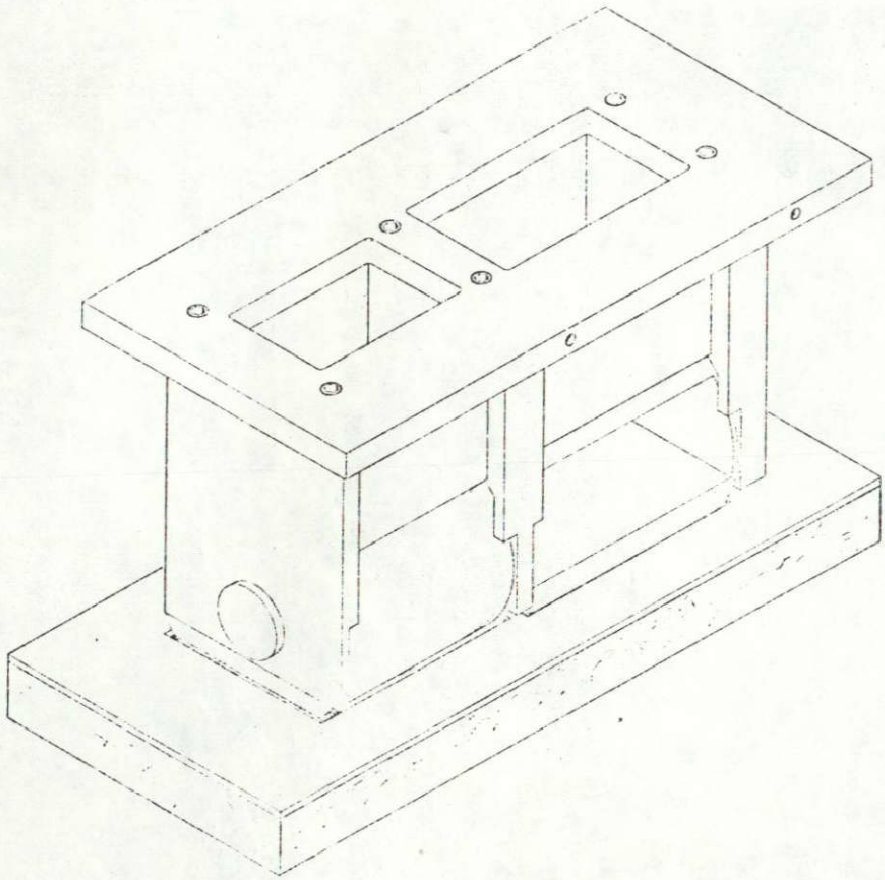

Fig. 14. Schematic illustration of cylindrical trap doors in place over top of hot zone. Door at left is in open position; door at right is closed.

doors are in the form of a cylinder with a horizontal axis of rotation. In the "closed" position, two opposite quadrants of this cylinder act as doors, one mating to the top of the top plate, the other to the top of the hot zone. In this configuration, atmosphere is kept from entering the furnace by one quadrant, and the opposite quadrant keeps hot furnace gases in the hot zone and acts as a radiation shield. A 90^{o} rotation of the cylinder brings the trap door to the open position, and the cartridge is inserted through the rectangular opening in the trap door cylinder between the two solid quadrants.

The 90^{o} rotation of the trap door cylinder is accomplished via an argon powered vane motor built into the trap door support. These details are revealed in Fig. 15, a photograph of the two-station trap door assembly from Machine 17 (the entire assembly is inverted in this photograph). Actuation is accomplished by admitting a stream of argon into the vane cavity through the top plate. Reversal is accomplished by admitting the argon to the other side of the vane pump.

These trap doors have registered reliable operation as not a single run has been lost or compromised on their account. This concept represents a clean and simple solution to the problem of trap doors, especially important to the operation of a multiple furnace.

With its slide-out hot zone, cylindrical trap doors, overhead cartridge, and puller support structure (see Fig. 16), and provision for melt replenishment cartridge, Furnace 17 is, in fact, a single ribbon "multiple" growth production furnace. Thus, any knowledge derived from it and any technology developed on it will be immediately transferable to a real production multiple growth furnace.

C. Instrumentation

Traditionally, crystal growth has been viewed through tele-microscopes. In EFG growth of 7.5 cm wide ribbon, the meniscus is 7.5 cm wide, but only about .02 cm high. Thus, the viewer must select a magnification that allows him to resolve the small meniscus height and scan continually over the width of the ribbon. While such a system is acceptable for growth of a single ribbon, it does not lend itself readily to any means of video recording and hence instrumentation, and, more important, it puts a severe strain on the operator of a multiple growth furnace.

The solution to this problem, as implemented on Machine 17, is the design of an optical system which enlarges the image more in the vertical

Fig. 15. Partially assembled cylindrical trap doors. Note detail of vane cavity. Assembly is inverted from normal position.

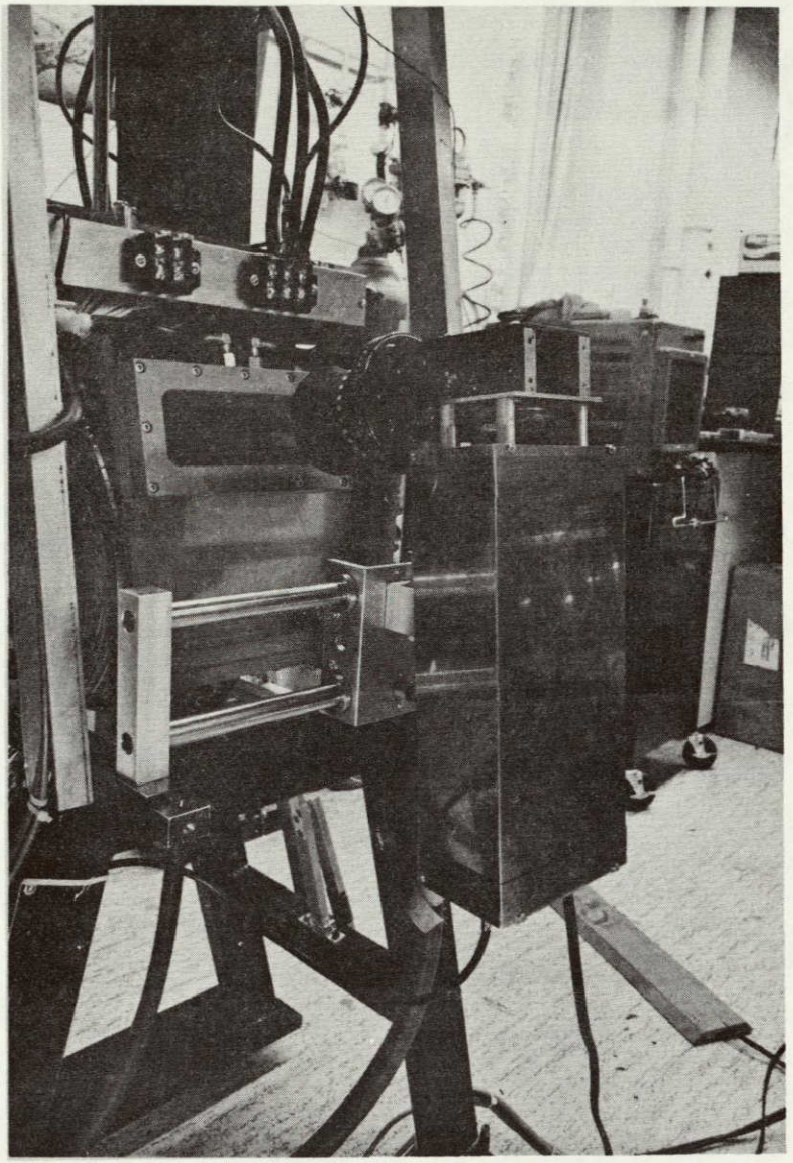

Fig. 16. Anamorphic optical-video system installed on furnace.

direction than in the horizontal, thus allowing for good vertical resolution while keeping the full ribbon width in view. The anamorphic optical-video system which accomplishes this task is shown in Fig. 17. It consists of a collimating lens, six prisms, a TV lens, and a TV camera. As may be seen from the photograph, its overall size is about the same as that of a standard microscope.

Figure 18 presents a photograph taken directly from the TV monitor. The top two-thirds of the image is the view of the growth as seen by the anamorphic optical-video system. The die, meniscus, and ribbon are indicated on this photograph. In this case, a 2.5 cm wide ribbon is being grown from a 7.5 cm wide die. Note that excellent resolution is maintained on the .025 cm high meniscus, while the full 7.5 cm wide die is in view.

The bottom one-third of this split-screened image presents the instrumentation panel as seen by the second TV camera. Here, the relevant growth data are presented in a format that allows the grower quick reference. The instrumentation package itself is highly versatile so that variation of the display of parameters is easily accomplished.

This optical-video system is useful in three respects.

1. It represents the key to the utility of Machine 17 as an instrumental furnace as it allows for the video taping of the growth process and the relevant growth data. This permanent record has already proven its utility in investigative work.

2. It affords the operator a means of viewing EFG, which at the same time provides more information on meniscus heights, and reduces operator fatigue. The cost of this optical-video system (even in unit quantities) is comparable to that of a high quality microscope, and few improvements need to be made before a state of production worthiness may be declared for this device. As such, the anamorphic optical-video system is of great potential value in multiple growth operations.

3. Perhaps the most important feature of this system is its adaptability to automatic control. Some simple, off-the-shelf video analysis equipment has already shown that the information needed for control of the ribbon dimensions (namely edge positions and meniscus height) may easily be obtained directly from the video image. Thus, this system may be viewed as the beginning of an interactive automatic control system where ribbon edge position and meniscus height may be used to control the cartridge heater power levels.

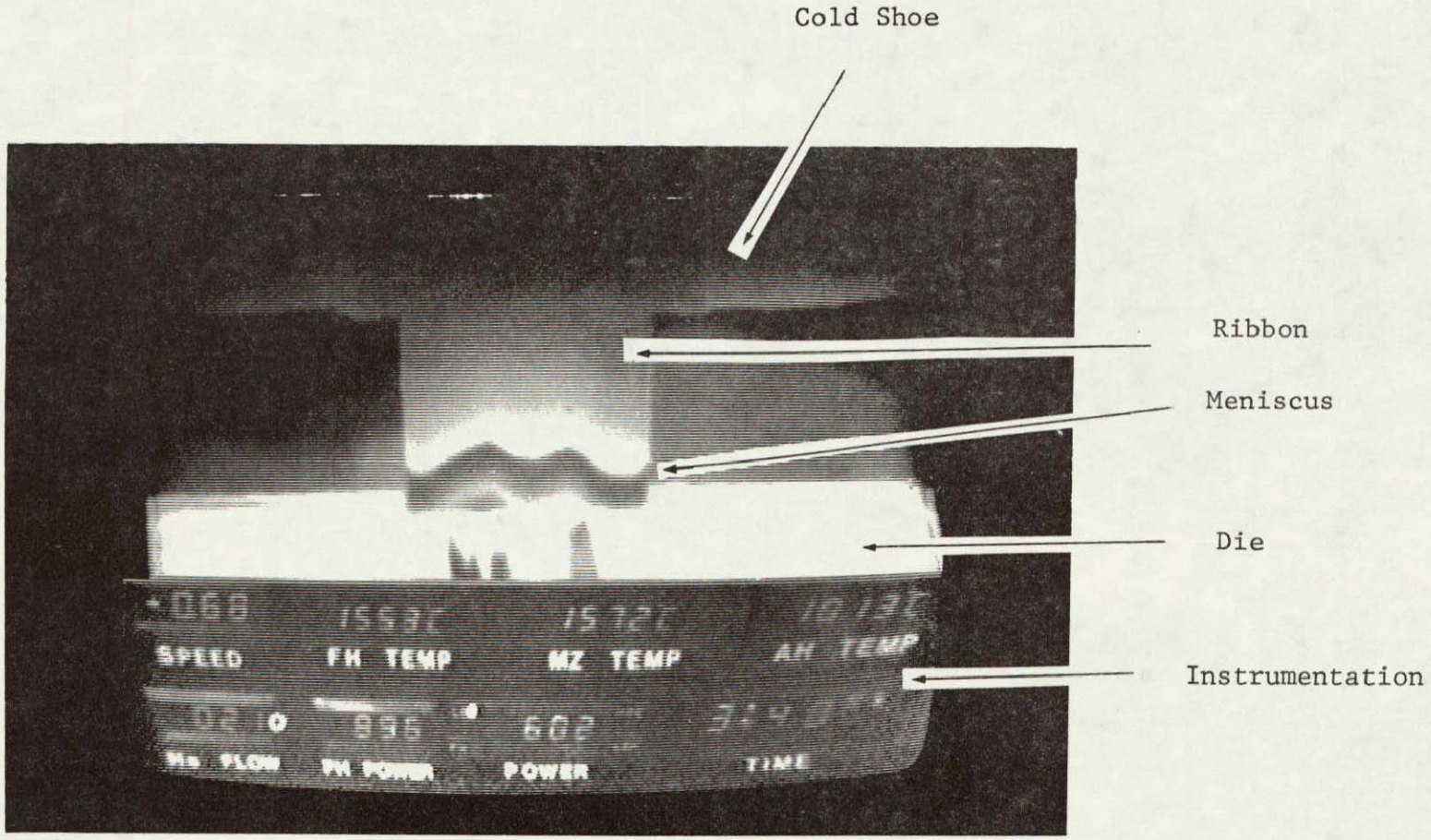

Fig. 17. Photograph of full TV image of a section of 2.5 cm wide ribbon taken in the "pause" mode (see text for details).

D. Growth System Design

It is a measure of the progress on the JPL program in general that we are now in a position to devote considerable effort to investigations of the effect on growth of variations to the cartridge elements near the die. Wraparound end heaters, bulbous dies, different shield configurations, and different variations of cold shoes are some of the efforts carried out to date.

Among these efforts is the introduction of the mini cold shoe in the 7.5 cm cartridge. The purpose of the mini cold shoe was to achieve a higher degree of isolation between the thermal modifier elements in the cartridge by minimizing the heat transfer between them. Experiments have shown that these heat interactions have, in fact, been reduced by up to a factor of 3 depending on the amount of helium flowing through the cold shoe. These measurements were made with no radiation shields between mini cold shoe and afterheater, while the standard cold shoe uses five shields.

In five growth runs in Machine 18, little difference in growth performance has been noted between mini and standard cold shoes. However, we believe that suitable tailoring of the mini cold shoe will play a role in stress reduction effects as it will facilitate finer control over the temperature profile, as seen by the ribbon through reduced thermal interactions.

E. Experiments to Date

To date, four growth runs have been made. The first two were made with the mini cold shoe and grew approximately 2 m of 3 - 7 cm wide ribbon each. These runs were largely shakedown runs for the entire system.

The third and fourth runs were made without a cold shoe. The motivation for running without a cold shoe is threefold.

1. The sensitivity of EFG to thermal perturbations in general increases as the system growth speed decreases. As such, a low growth speed system with no cold shoe makes thermal imbalances at the die top more apparent. Hence, growth with no cold shoe represents a good way to test and tune the die thermal modifiers.

2. The cold shoe represents a possible source of contamination. Hence, growth without it provides an important piece of information as to material quality (once performed on a clean system).

3. The simple growth system without the cold shoe will provide a good starting point for thermal stress studies.

Both runs to date without the cold shoe have been moderately successful with approximately 1 to 2 m of 4 to 7 cm ribbon grown in each. The second was somewhat handicapped by oxygen or water vapor contamination of the argon.

The last two runs have been made with an antimony doped melt for the purpose of attempting to demarcate the interface by freezing-in the boundary layer of impurities accumulating in front of the crystallization front. Antimony was chosen as it has proven successful (it has low segregation coefficient and is easily revealed by etching) in Peltier pulse interface demarcation with CZ growth.[7]

The problems introduced by arcing between the ribbon and the after-heater make Peltier pulsing extremely difficult to envision in our growth systems; hence, we are forced to resort to single speed pulsing by hitting the belt puller.

Figures 18 and 19 show the interface demarcation obtained by this technique during one of the runs without a cold shoe. Actually, it appears that inherent vibrations in the system were sufficient to cause the boundary layer to freeze-in, hence the close spacing of the interface lines. The occasional intentional speed pulse merely shows as an exaggerated marking. Partial melt-back of lines is also apparent in these photographs.

The interface markings are seen to be only slightly concave down, as is expected in a low growth speed system with no cold shoe. The higher magnification view of Fig. 19 shows the interface responding to grain boundaries, etc., in a cusp-like manner.

It is hoped that this technique will prove useful in studying displaced dies and structure formation in general, especially in combination with observed interface cusping in the video tapes of growth.

From these four growth runs, it is felt that there are no fundamental obstacles to good reliable growth being shortly attained. Seeding conditions were acceptable to good in all cases, and we are hampered primarily by lack of experience in running the system compounded by some final electronic power controller problems that were left to be sorted out.

It is our intention to continue to run the system with no cold shoe to a point of reliable 7.5 cm wide growth while beginning investigations of:

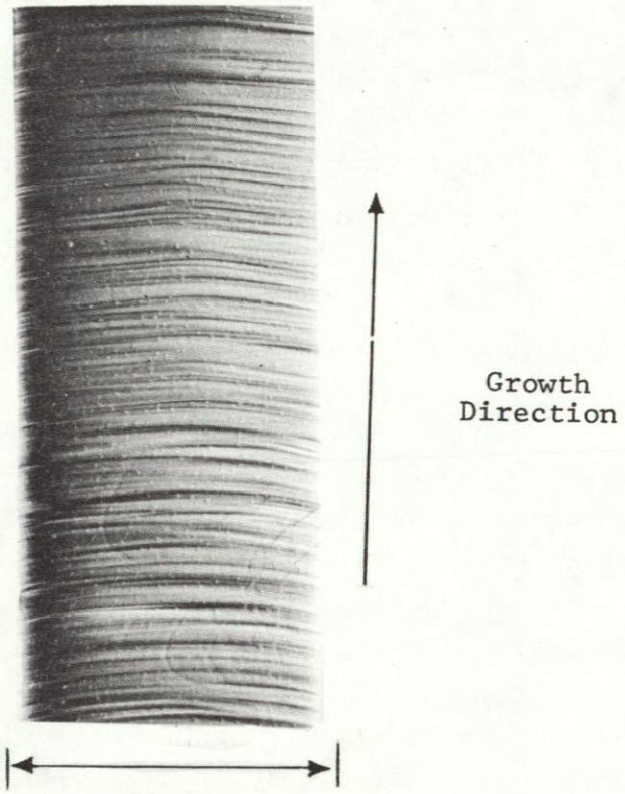

Fig. 18. Longitudinal cross-section of antimony doped ribbon showing interface markings. Interface is delineated by freezing in of antimony and subsequent etching (65X).

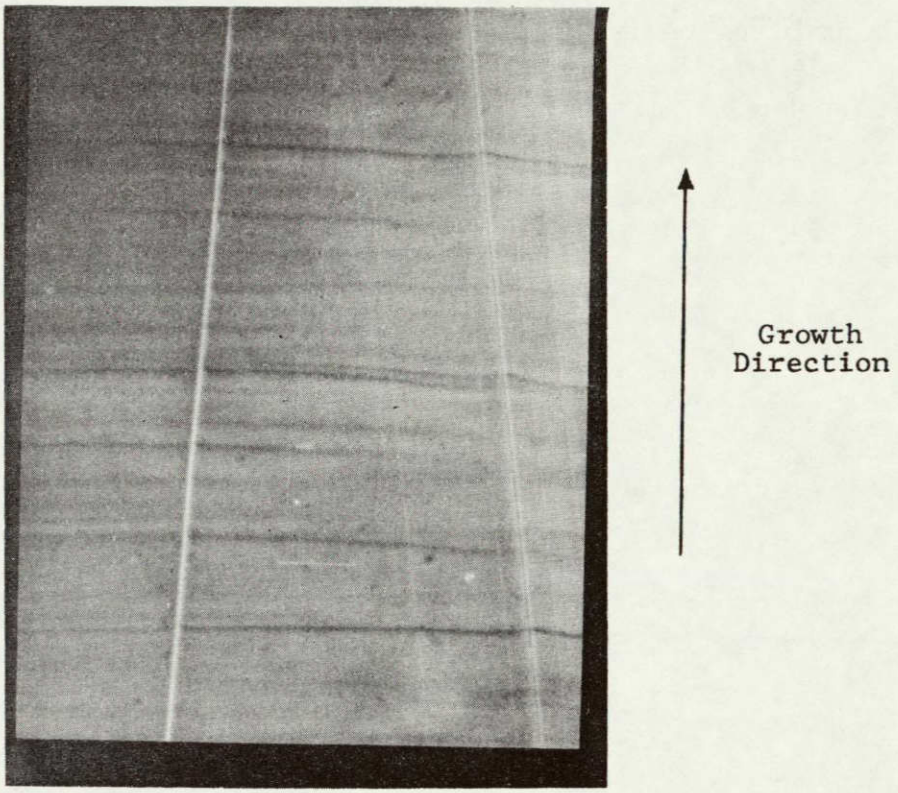

Fig. 19. Closeup view of interface markings (225X) showing interaction of interface with structural features in ribbon.

1. Thermal stresses - using ribbon thermocouples, and standard thermocouples to characterize the thermal environment and correlate it to buckling tendencies.

2. Causes of spreading and tapering - primarily by studying video tapes of the growth and correlating meniscus shapes with spreading tendencies.

3. Growth dynamics and controllability - studies leading to the direct control of meniscus height.

VI. REFERENCES

1. F.V. Wald et al., "Large Area Silicon Sheet by EFG," Second Quarterly Progress Report, DOE/JPL 954355/78-2 (July 1978).

2. J.P. Kalejs, "Impurity Redistribution in EFG," J. Crystal Growth, 44 (1978) 329.

3. F.V. Wald et al., "Large Area Silicon Sheet by EFG," Annual Progress Report, ERDA/JPL 954355/77-3 (September 1977).

4. F.V. Wald et al., "Large Area Silicon Sheet by EFG," Fourth Quarterly Progress Report, DOE/JPL 954355/77-4 (January 1978).

5. E.M. Pell, "Interaction Between Li and O in Si," Solid State Physics in Electronics and Telecommunication, Vol. 1, p. 261, Academic Press (1960).

6. K. Graff et al., in: Semiconductor Silicon, Ed. H.R. Huff and E. Sirtl, The Electrochemical Society, Princeton, N.J., p. 575 (1977).

7. M. Lichtensteiger, A.F. Witt, and H.C. Gatos, J. Electrochem. Soc., 118 (1971) 1013.

APPENDICES

1. Updated Program Plan

   See attached chart.

2. Man Hours and Costs

Previous cumulative man hours were 49,883 and cost plus fixed fee was $1,776,136. Man hours for the third quarter of 1978 are 6,968 and cost plus fixed fee is $235,163. Therefore, total cumulative man hours and cost plus fixed fee through October are 56,851 and $2,011,200, respectively.

3. Engineering Drawings and Sketches Generated During the Reporting Period

   Section III.C, Fig. 11; Section V.B, Fig. 14.

4. Summary of Characterization Data Generated During the Reporting Period

Section II.B.2, Table II, Figs. 3 through 10; Section III.B, Tables III and IV; Section III.C, Tables V, VI, VII, and VIII. General: Section IV as a whole demonstrates the achievement of large area (2.5 x 7.5 cm^2) cells with efficiencies between 9 to 10% AM1.

5. Action Items Required by JPL

   None.

6. New Technology

New technology items have been separately reported for patent action.

APPENDIX 1

Updated Program Plan for 1978

Machine No.		May	June	July	Aug	Sept	Oct	Nov	Dec
JPL No. 1 (18)	Initial Quality Baseline	1.5"/min							
	Material Quality Studies								
	Die Design								
	Buckles/Ripples Guidance				1.5"/min				
	3"/min								
JPL No. 3A (16)	Ribbon Quality	Graphite / Quartz							
	3"/min System Test		Exist. Cart.						
	Melt Replenishment/Dopant/Purity								
	Multiple Hot Zone } Design / Assembly								
	Multiple Growth								*
17	Machine Construction								
	Buckles and Stress in High Speed Growth								
	Growth Stability								
	Freeze Mechanisms								
	Interface Shape	When Slack Occurs							
	Characterization								

*Multiple growth is to start only if 7% efficiency has been exceeded on single ribbons from the "short hot zone".